



UNIVERSITÀ DEGLI STUDI DI PADOVA

**DIPARTIMENTO DI BIOMEDICINA
COMPARATA ED ALIMENTAZIONE**

Corso di Laurea Magistrale in
Biotecnologie per l'Alimentazione

**System for *Listeria monocytogenes*
detection in milk**

Relatore: Prof. Fabio Vianello

Correlatori: Dott. ssa Emanuela Bonaiuto
Dott. Luca Fasolato

Laureanda: Maddalena Varotto
1109116

ANNO ACCADEMICO 2016/2017

“Al servizio di tutti, servo di nessuno”

Papà

TABLE OF CONTENTS

INTRODUCTION

CHAPTER 1

Biosensor evolution and nanoscience

1.1. Biosensors	pag. 1
1.1.1. Main features of the ideal biosensor.....	pag. 4
1.1.2. Biosensors classified according to the type of biological element (receptor).....	pag. 7
1.1.3. Biosensors classified according to the technique used for signal transduction.....	pag. 9
1.2. Nanoscience and Self-Assembled Monolayer (SAM) ...	pag. 10
1.3. Biotin - avidin system	pag. 14
1.3.1. Biotin.....	pag. 14
1.3.2. Avidin.....	pag. 17
1.3.3. Applications of the biotin-avidin system.....	pag. 18

The importance of food safety and the detection of pathogenic *L. monocytogenes* in milk

1.4. Food safety	pag. 21
1.5. <i>Listeria monocytogenes</i> and listeriosis	pag. 22
1.5.1. Discover of <i>L. monocytogenes</i>	pag. 22
1.5.2. Molecular and taxonomical profile of <i>L. monocytogenes</i>	pag. 23
1.5.3. Listeriosis.....	pag. 27
1.6. Classical methods for <i>L. monocytogenes</i> detection and enumeration	pag. 29
1.6.1. Qualitative and quantitative methods for detecting <i>L. monocytogenes</i>	pag. 29
1.6.2. Molecular methods for detecting <i>L. monocytogenes</i>	pag. 31
1.6.3. Immunological methods for detecting <i>L. monocytogenes</i>	pag. 32

1.7. Innovative methods for <i>L. monocytogenes</i> determination.....	pag. 33
1.7.1. Micro-gravimetric biosensor.....	pag. 33
1.7.2. Biosensing and magnetic nanoparticles.....	pag. 35

AIM OF THE PROJECT

CHAPTER 2.....	pag. 39
-----------------------	---------

MATERIALS AND METHODS

CHAPTER 3: The preparation of bacterial culture and instrumentation to detect *L. monocytogenes* in milk

3.1. Reagents and solvents applied.....	pag. 41
3.2. Preparation of inactivated <i>L. monocytogenes</i> inoculums.....	pag. 43
3.3. The piezoelectric system.....	pag. 44
3.4. SAMNs.....	pag. 47
3.4.1. Synthesis of SAMNs.....	pag. 47
3.4.2. Derivatization of SAMNs with avidin and Ab- <i>L. monocytogenes</i>	pag. 48
3.5. Tests for <i>L. monocytogenes</i> capture.....	pag. 49
3.5.1. Citotoxicity test to evaluate the effects of SAMNs on <i>L. monocytogenes</i>	pag. 49
3.5.2. <i>L. monocytogenes</i> capture experiments with bare SAMNs and SAMN@Av@Ab- <i>L. monocytogenes</i> in PBS.....	pag. 50
3.5.3. Capture test with different concentration of SAMN@Av@Ab- <i>L. monocytogenes</i> in PBS and in milk.....	pag. 54

RESULTS AND DISCUSSION

CHAPTER 4: Effectiveness of the new immunosensor in detecting *L. monocytogenes*

4.1. Antibody immobilization on piezoelectric quartz crystal and response to mass addition of <i>L. monocytogenes</i>.....	pag. 57
4.1.1. Derivatization of crystal surface and the qualitative method to detect <i>L. monocytogenes</i>	pag. 57
4.1.2. Amplification of piezoelectric signal of <i>L. monocytogenes</i> by the SAMN@Av@Ab- <i>L. monocytogenes</i>	pag. 63
4.1.3. Reduction of the incubation time of SAMN@Av@Ab- <i>L. monocytogenes</i> and <i>L. monocytogenes</i>	pag. 69
4.1.4. Test of the antibody specificity for <i>L. monocytogenes</i> ...	pag. 71
4.2. Interaction of SAMNs with live <i>L. monocytogenes</i> and capture efficiency of SAMN@Av@Ab-<i>L. monocytogenes</i>.....	pag. 74
4.3. Capture of <i>L. monocytogenes</i> in PBS: preliminary experiments with SAMNs and SAMN@Av@Ab-<i>L. monocytogenes</i>.....	pag. 76
4.4. Capture test with different concentrations of SAMN@Av@Ab-<i>L. monocytogenes</i> on milk samples...	pag. 79
CONCLUSIONS.....	pag. 81
BIBLIOGRAPHY.....	pag. 83
ACKNOWLEDGMENTS.....	pag. 97

INTRODUCTION

CHAPTER 1

Biosensors evolution and nanoscience

1.1. Biosensors

Two of the most important scientific discoveries of the Modern Era are the understanding of the chemical mechanisms governing the acid-base reactions and the comprehension of some crucial aspects of the biological systems, based on a series of studies regarding the interactions between biomolecules and their characterization through the analysis of the structure-function relationship.

In 1909, the Danish scientist Sørensen defined the concept of pH with its scale and, through subsequent studies, he concluded that the pH plays a key role in chemical and biochemical processes [1]. Just three years later Michaelis and Davidoff used an electrode to measure the pH of lysed red blood cells, while in 1927 Buytendijk used it for the first time for biomedical purposes [2]. The measurement of blood pH – which has become a routine clinical examination – highlighted the important role played by H^+ ions in respiration and metabolism processes.

Further advancements in electrochemistry are connected to the work of Heyrovský, Nobel prize for Chemistry in 1959 and inventor of the Dropping Mercury Electrode [3], who measured the redox potential of different chemical species. This particular electrode was also used to analyse a series of elements in biological matrices. However, its use evidenced the need for different methods of analysis, stable over time, reproducible, and not requiring frequent calibrations and/or large amounts of samples. As a result of several modifications and considerable improvements, in the mid-fifties the american biochemist and physiologist Clark Jr. patented a sensor able to measure the dissolved oxygen in the blood, and later he managed to immobilize the glucose oxidase enzyme on an oxygen sensor [4], developing a valid tool for measuring the concentration of glucose in the blood.

In recent years, it became necessary, both at the social and scientific level, to identify novel strategies and new measurement methods for quantitative determination of natural and artificial chemical species, in order to assess and monitor their spread in the environment and their effects on living organisms [5]. This stimulated the development of chemical sensors and, more recently, of biosensors. The term “chemical sensor” refers to a device capable to provide quantitative or semi-quantitative information regarding the presence of a given analyte in a certain environment, by means of returning a proportional signal on the molecule concentration of the analyte under examination. Usually the components of the sensor are two: **(a)** a receptor, which causes a chemical reaction that involve the analyte, and **(b)** a chemical-physical transducer, which turns the receptor’ chemical modifications into an electrical signal. If the transducer is an electrode,

the output signal is electrochemical in nature and, consequently, the sensor itself is defined as a chemical (or electrochemical) one.

A chemical sensor that contains a biological element at the receptor level is defined biosensor [6]. Some distinctive features of biosensors are: **(a)** the ability to recognize and respond to specific chemical substances (high selectivity); **(b)** ease of use by operators; **(c)** rapid response times; **(d)** high reproducibility, and **(e)** their low cost. The biosensor's main components (**Fig. 1.1.**) can be described as follows:

- 1) Receptor. It is the component that allows the recognition process and the onset of specific interactions between molecules, imitating the events that normally occur in biological systems [6]. It can be constituted by any type of biological element (such as enzymes, proteins, antibodies, nucleic acids, cells, tissues or whole organisms) [7]. The biological element defines the specificity of the biosensor.
- 2) Transducer. It is the physical element that transforms the biochemical modification occurring after the molecule-receptor interaction into a detectable signal (electrical, electrochemical, optical, gravimetric, colorimetric, etc.).
- 3) Detection system and signal processing. It is a necessary component in order to process the data obtained from the output signal, generally consisting of a signal conditioning system, a display, a processor and a storage system.

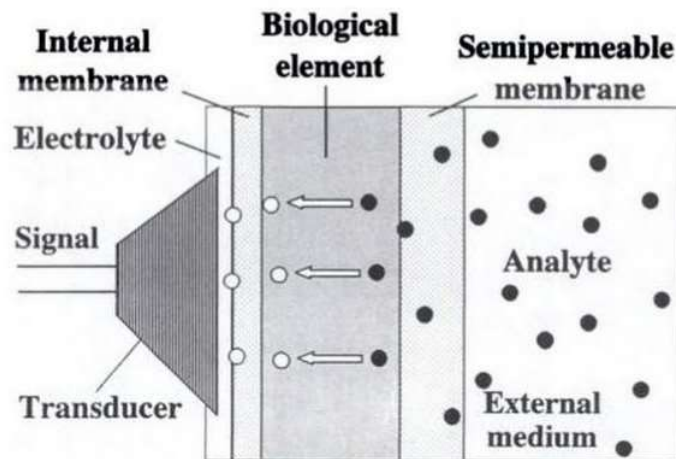


Fig. 1.1. Simplified of a biosensor [2].

1.1.1. Main features of the ideal biosensor

There is an endless variety of biosensors, which show different structures but ground their action mechanisms on the same scientific foundation [5]. The differences between biosensors depend primarily on the properties of the measuring system and on the environment in which the measurement is carried out. Some of the functional features of the ideal biosensor are presented below.

Sensitivity. The International Union of Pure and Applied Chemistry (IUPAC) defines sensitivity as «the slope of the calibration curve. If the curve is in fact a 'curve', rather than a straight line, then of course sensitivity will be a function of analyte concentration or amount. If sensitivity is to be a unique performance characteristic, it must depend only on the chemical measurement process, not upon scale factors» [8] (**Fig. 1.2.**). Generally, what is directly detected by the biosensor

is not the analyte itself, but the difference in concentration of the chemical species produced as a consequence of the interaction between the analyte and the biosensor. The measurement of some biosensors depends on the biosensor dynamic response, therefore the sensitivity may be understood as the signal change with time for a given variation in concentration ($\Delta S \Delta t^{-1} \Delta C^{-1}$, where S is sensitivity, t corresponds to time and C indicates the concentration). Ideally, the biosensor should keep its sensitivity constant in time, allowing for a correct signal detection.

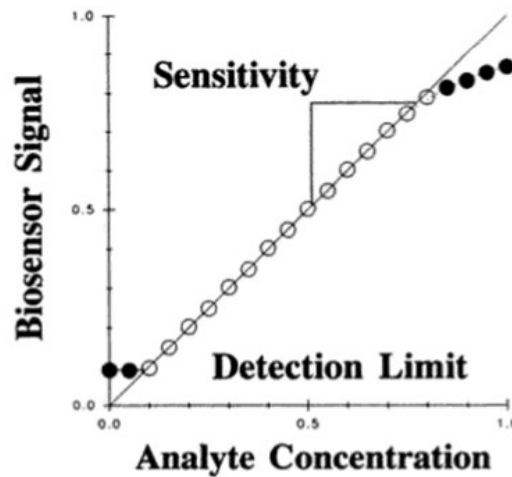


Fig. 1.2. Biosensor's sensitivity [2].

Calibration. It is a necessary operation for improving the accuracy of the instrument and its measurement. The biosensor can be calibrated simply by the exposure to standard solutions containing different known analyte's concentrations. Ideally, the values of the measurements to be made should be abundantly contained in the range of points identified by the calibration, so that the measurements remain

into the given range. It is necessary that the instrument is calibrated periodically and regularly with time to verify that in the long run no changes of sensitivity take place.

Limit of detection. Ideally, the analyte's lowest concentration detectable by the biosensor should be limited only by the resolution of the instrument (**Fig. 1.2.**). Actually, however, there are different factors that can generate interferences in the measurement, and consequently heighten the limit of detection.

Selectivity (interference). An ideal biosensor should respond only to changes of analyte's concentration and shouldn't be influenced by the presence of another chemical species. In practice, however, this is not possible. Since the control of the chemical species that cause the interference is not easy, it is useful to measure them with another type of transducer, in order to correct the signal produced by the biosensor.

Temperature dependence. Enzymatic reactions depend on temperature. This aspect cannot be underestimated, because in an environment in which different chemical reactions occur, heat is likely to develop. Heat can change the biosensor's temperature, thus invalidating the measurement. Limiting the measurements in isothermal conditions, e.g. using a water-bath, is a good practice

Lifetime. The biosensor should be stable under normal operational conditions during its lifetime. The lifetime of the biosensor should be limited as a consequence of **(a)** several measurements performed; **(b)** high analyte concentration, or **(c)** chemical species produced. The biosensor must be maintained in a refrigerated

environment or under particular chemical conditions, in order to preserve it between one measurement and the subsequent one.

1.1.2. Biosensors classified according to the type of biological element (receptor)

According to the type of biological element constituting the receptor, biosensors can be distinguished into five major categories [7], which will be briefly described below and shown in **Fig. 1.3**.

- 1) Antibody-antigen based. These biosensors operate on the basis of the binding of an antigen to a specific antibody, forming antibody-antigen complexes detected under conditions, in which non-specific interactions are minimized.
- 2) Enzymes based. For their catalytic activity, certain enzymes require a cofactor, while others do not need further chemical groups in addition to their amino acid residues. In the biocatalytic recognition mechanism, the activity of enzymes depends on the integrity of their native protein conformation: a denatured enzyme has not a catalytic activity.
- 3) Nucleic acids based. These biosensors are called also DNA biosensors, genosensors or biodetectors. They are used to identify small concentrations of DNA in a large sample, on the basis of the comparison between a DNA in the sample with a known DNA immobilized on the transducer.

- 4) Cellular structures based. Biosensors with whole cells as a biological element have the ability to detect organic and inorganic compounds, as well as stress conditions, toxicity and DNA damaging agents. These biosensors are used also to test and control the effects of drugs and toxins.
- 5) Biomimetic materials based. These can be called “synthetic biosensors”, because they are made of materials created in laboratory, such as aptamers or PNA. Aptamers are artificial nucleic acid ligands generated against amino acids, drugs, proteins and other molecules. PNA is a synthetic DNA analogue-peptide, that can bind with high affinity to its complementary nucleic acid sequence of DNA.

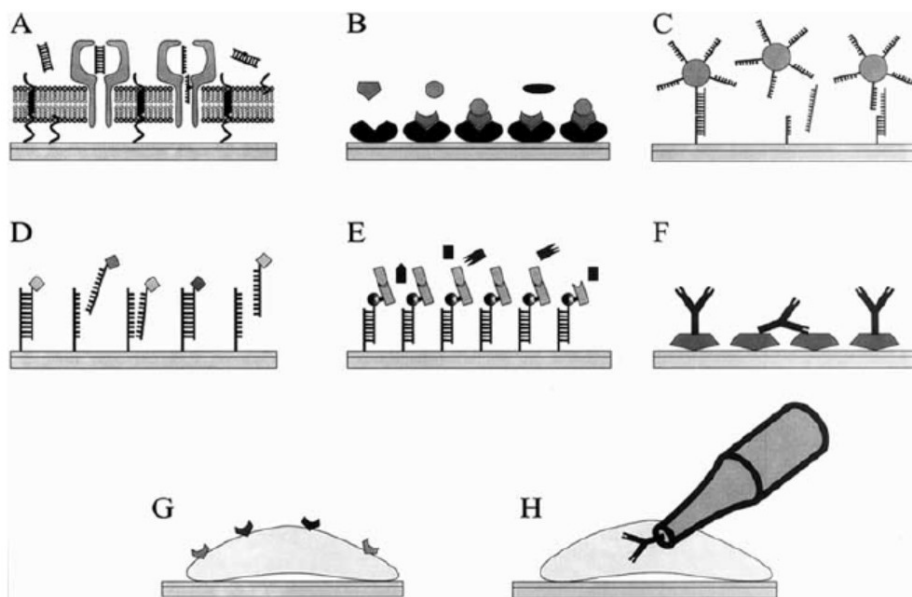


Fig. 1.3. Biosensors classified according to the type of biological element composing them [7]. **A:** transmembrane (nanopore) sensor; **B:** biocatalytic (enzyme) sensor; **C:** DNA based sensor, hybridisation with nanobead labelled oligonucleotides; **D:** DNA based sensor, hybridisation with fluorescent labelled

oligonucleotides; **E**: DNA based sensor, detection of hybridised oligonucleotides carrying a given antigen by the antigen specific antibodies; **F**: antibody sensor with immobilized recognition proteins; **G**: sensor utilizing cells to monitor cell's processes by an extracellular detection or **H**: intercellular detection system.

1.1.3. Biosensors classified according to the technique used for signal transduction

According to the technique used for signal transduction, biosensors can be distinguished into four major categories [7], which will be briefly described below.

- 1) Optical-detection biosensor. It can be used for many types of spectroscopy, such as luminescence, absorption, polarization and fluorescence, with different spectrochemical properties recorded, such as amplitude, energy, polarization, decay time and/or phase.
- 2) Electrochemical biosensor. It measures electrical property of electrochemical reactions. Amperometric biosensor correlates the current resulting from the electrochemical oxidation (or the reduction) of an electroactive species with the bulk concentration of the electroactive species. On the other hand, conductometric biosensor employs ion conductometric or impedimetric devices based on the use of integrated electrodes for monitoring various enzymatic reactions and biological membrane receptors.

- 3) Biosensor based on mass-sensitive measurement. By means of measuring the crystals' oscillation frequency, it is possible to measure indirectly small changes in a mass of the crystal due to binding of chemicals species.
- 4) Thermal-detection biosensor. It measures the heat generated by enzyme and analyte reactions.

1.2. Nanoscience and Self-Assembled Monolayer (SAM)

The purpose of nanoscience is to study objects and systems in a range size of 1-100 nm, i.e., objects larger than atoms but smaller than the structures generally used in microtechnology (microfluidic, microelectronics, etc.). In nature, nanostructured materials are synthesized by means of biomineralization, a formation process of inorganic crystals or amorphous particles in biological systems [9]. In addition to that, chemists have developed synthetic methods for producing uniform nanostructures of 1-100 nm with new shapes and/or compositions, aiming at applying these structures with different purposes in medicine, in magnetic storage media and in optical and electronic devices [10]. Nanostructures have the great part of their constituent atoms on the surface and their physical properties, substantially different from those observed in bulk materials, depend on the extent of their surface. The interfacial environment and Self-Assembled Monolayers (SAMs) offer a versatile and simple system fitting the interfacial properties of metals, metal oxides and semiconductors [10].

In 1930, Langmuir and Blodgett demonstrated that monolayers of surfactants can be transferred onto solid substrates to form stable films, known as “Langmuir - Blodgett films” [11]. In 1946, when Zisman introduced a possible alternative to the Langmuir-Blodgett system describing the preparation of a monomolecular layer by means of adsorption of a surfactant onto a clean metal surface [12], there was a mild interest in the possible application of self-assembly techniques. The recognition of the potential of molecularly organized films as advanced materials determined a renewed interest in this topic in the 1980s. In particular, the interest in monolayers of alkane-thiolates on gold surface was extensive. Gold is a good substrate for studying SAMs because it is an inert metal easy to obtain, it is used in a great number of spectroscopic and analytical techniques, and cells can adhere to it without evident toxicity. However, several research groups extended SAMs beyond the prototype gold/thiol system, using for example fatty acids on aluminium [13], silanes on silicon [14] and phosphates on metals [15]. The term “self-assembly” implies the spontaneous adsorption of molecules/nanoparticles onto a substrate, consequently “self-assembled multilayer films” are formed by the adsorption of subsequent monolayers of molecules/nanoparticles. Thiols have high affinity for the metals surfaces, in particular for gold [16], and they can generate well-defined organic surfaces with a typical thickness of 1-3 nm, showing interesting chemical functionalities at the exposed interface [10]. The process of multilayers self-assembling of surfactants is characterized by sequential steps:

- 1) adsorbing thiol surfactants on the metal surfaces;
- 2) chemically linking the second layer of surfactants to the anchored monolayer;

3) repeating step 2) for a given number of times.

Monolayers and self-assembled films are not constructed exclusively by surfactants, indeed the methodology extends to larger molecules, in order to form films from fullerenes, polyelectrolytes (**Fig. 1.4.**), polystyrene microspheres, silylated glass beads and surfactant-coated metallic, semiconductor, magnetic, and ferroelectric nanoparticles [17].

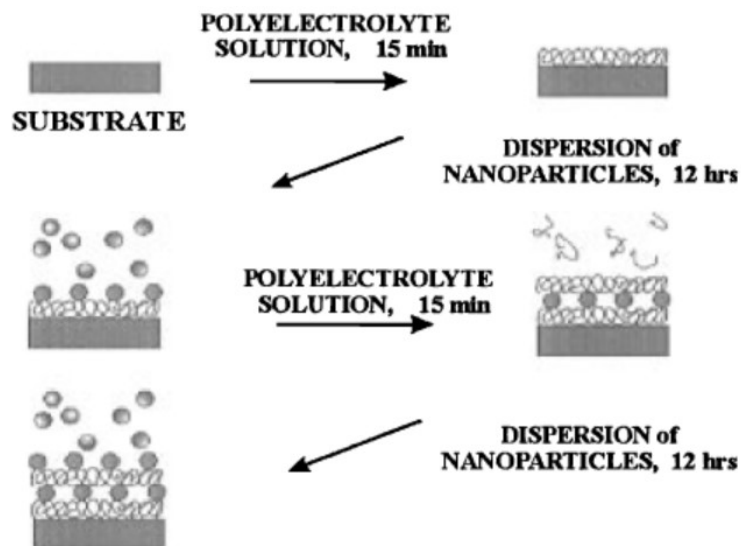


Fig. 1.4. Schematic representation of the self-assembly of an S-(P/Cds)_n film [17].

SAMs are very important in nanoscience due to several reasons:

- 1) they are easy to prepare;
- 2) they form object of any size and are critical elements for stabilizing and adding new functions to them;

- 3) they can relate the external environment to the properties (e.g., electronic or optical) of metallic structures;
- 4) they link macroscopic interfacial phenomena to molecular level [10].

It is important to note that SAMs may provide the control of the molecular order, since the molecules can be set in a specific orientation with respect to the metal [18]. It is desirable to assemble individual molecules into highly ordered architectures. In the final equilibrium structure of the assembly, the interactions between substrate and adsorbate, electrostatic and Van der Waals forces, as well as intramolecular interactions play a key role [19]. Controlling the properties of interfaces is a crucial aspect for many applications and, in these cases, it is necessary to have an extensive database of detailed correlations between these properties and the structure of the polymer surface. Furthermore, SAMs constitute a connecting bridge between different research areas, such as physics, chemistry and biology, thanks to their biomimetic and biocompatible nature [20].

In this context, the complex chemical pathways that regulate the biological systems offer many examples of nanostructures and suggest new strategies to build artificial nanosystems. These allow, for example, to immobilize proteins on solid supports (**Fig. 1.5.**), and this is an important application in diagnostic and experimental biology [21].

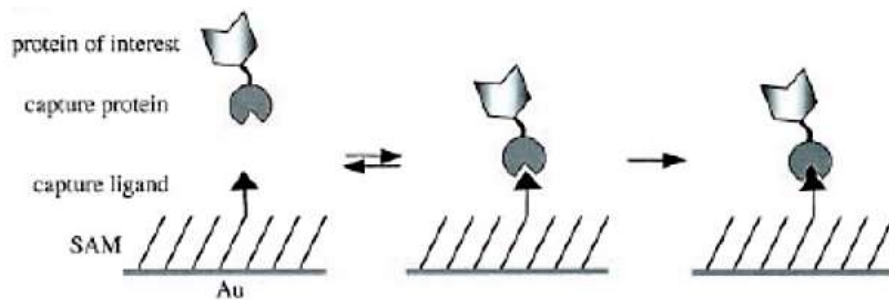


Fig. 1.5. Strategy for protein immobilization [21].

Examples of the broad potential application of SAMs in technology and biotechnology are semiconductor surfaces patterning and their use with piezoelectric or with other chemical sensors.

1.3. Biotin - avidin system

1.3.1. Biotin

Biotin (hexahydro-2-oxo-1 H-thieno[3,4-d] imidazole-4-pentanoic acid) (**Fig. 1.6.**) is a water-soluble vitamin with a molecular weight of 244,3 Da, isolated and characterized for the first time in 1936 by Kögel and Tönnes from duck egg yolk [22].

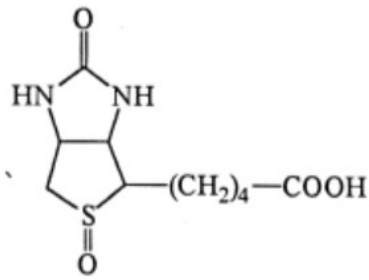


Fig. 1.6. Structural formula of biotin (vitamin H).

Many bacteria and higher plants synthesize biotin. However, several microorganisms and higher animals, for example mammals, are not able to do that and they must take it with from dietary sources. Biotin is largely diffused in natural foodstuff and its richest dietary sources include liver, kidneys, heart, pancreas, poultry, egg yolk and milk. Nevertheless, the absolute content of biotin of these sources is low when compared with the content of the majority of other water-soluble vitamins [23]. In humans, the dietary biotin intake considered adequate for healthy adults is 35 to 70 μg per day. However, certain population groups, such as pregnant and lactating women, may need increased biotin intake, while vegetarian diet does not seem to change the biotin status [24]. The very low concentration of biotin in nature put at risk the metabolic homeostasis of cells and, in order to ensure an adequate biotin supply, higher organisms have evolved a very efficient biotin cycle (**Fig. 1.7.**), through which intestinal microflora can provide biotin to the host organism.

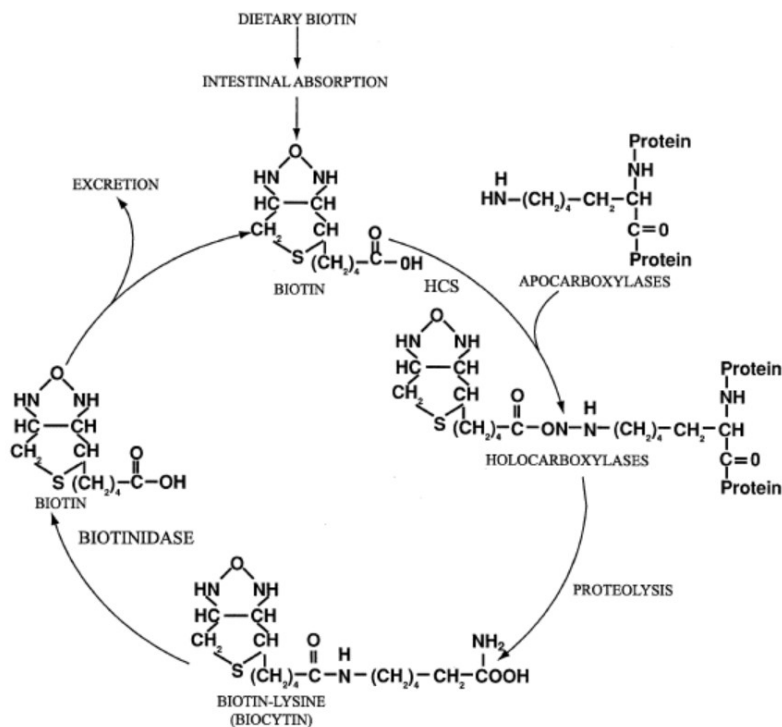


Fig. 1.7. Biotin cycle in mammals [25].

Most of the biotin contained in foods is protein-bound, and thus it must be released from the carboxylases to which it is attached before being used in carboxylation reactions. In human cells, biotin is a coenzyme of five biotin-dependent carboxylases, including propionyl-CoA carboxylase (PCC), pyruvate carboxylase (PC), methylcrotonyl-CoA carboxylase (MCC), acetyl-CoA carboxylase (ACC-1) and acetyl-CoA carboxylase 2 (ACC-2). These enzymes condition many physiological processes, such as the fatty acids synthesis, the gluconeogenesis and the amino acid catabolism [25].

Biotin plays different roles in metabolism and gene expression [26, 27]. Its deficiency can cause fatty acids insufficiency and this can impact the etiology of

cardiovascular diseases [28, 29]. Biotin starvation, as well as deficiencies of one of the abovementioned carboxylases, are associated with neurological manifestations, skin rash, hair loss, metabolic disturbances, protein malnutrition and, in pregnant women, it may be teratogenic [30].

1.3.2. Avidin

Avidin is a tetrameric glycoprotein of approximately 68 kDa, present in avian, reptilian and amphibian egg white, and comprising four identical subunits of 128 aminoacids [31] (**Fig. 1.8.**).

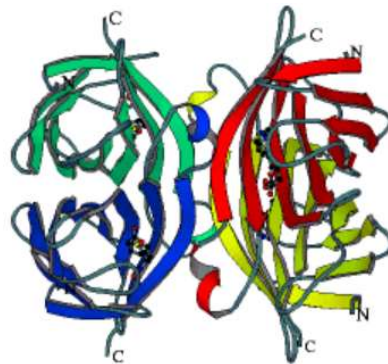


Fig. 1.8. Avidin structure: the four different colours show its four subunits, each of which can bind one molecule of biotin.

It has been found to be synthesized in chick oviduct and concentrated in egg white in response to a steroid hormone, progesterone [32], but, at the same time, it

was found also in many tissues independently of the presence of progesterone, following inflammations due to many causes, such as a toxic dose of actinomycin D, tissue traumas, bacterial sepsis or viral infections [33]. Its determination is very simple compared with the complex assays for other hormone-specific protein: indeed, it can be assayed directly in the tissue homogenate without any purification procedure [34]. No analogous protein has been detected in mammalian species [33], but several species of *Streptomyces* produce streptavidin, a protein with similar chemical and physical properties to avidin [35]. Nevertheless, these two proteins are clearly different. The biological function of avidin is not clear, but its capacity to bind biotin suggests it functions as an antimicrobial agent. In addition, it seems to represent a selective advantage for vertebrates [32].

1.3.3. Applications of the biotin-avidin system

The widespread interest for biotin in clinical and biomedical applications is generally due to a twofold reason:

- 1) The presence of a lateral chain, containing a carboxylic group, allows the biotin derivatization with a wide number of compounds, including antibodies, proteins and DNAs [36];
- 2) Avidin has high affinity for biotin: avidin can bind one molecule of biotin per subunits (**Fig. 1.9.**) in a very tight binding ($K_d = 10^{-15}$ M) [37] (**Fig.1.10.**).

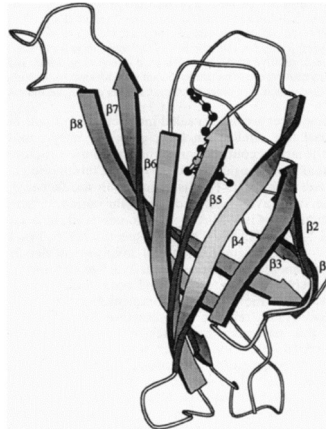


Fig. 1.9. Diagram of avidin-biotin monomer. Biotin is shown in balls and sticks model [38].

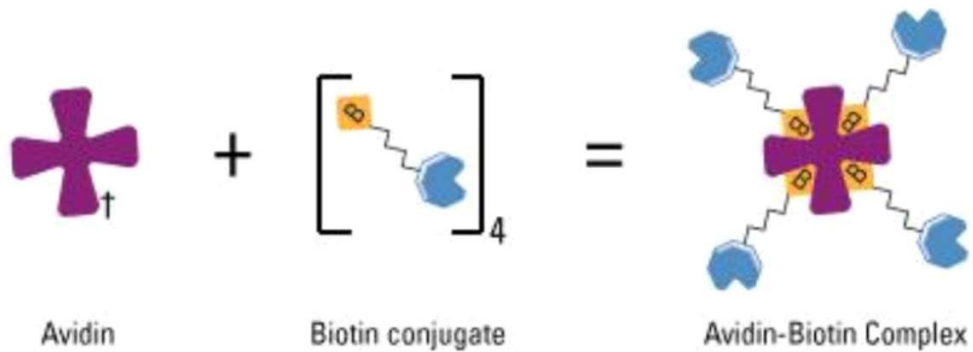


Fig. 1.10. Complex biotin-avidin formation.

The rapid and irreversible binding supports several applications for *in vitro* research. The interaction between biotin and avidin is a powerful tool for many analysis including quantitative enzyme immunoassays [39], selections and

purification schemes. In the field of nanoscience, the biotin/avidin system has been widely used in particular for protein immobilization, because, once biotin is on a molecular layer, it is very simple to immobilize any biomolecules with an avidin label. Thanks to the tetravalency of avidin for biotin, it is possible to construct a “molecular sandwich”, that allows the surface-bound avidin to be coupled with a biotinylated enzyme, with the adequate properties needed for the construction of a biosensor [40]. The interaction between biotin and avidin is highly resistant to a large quantity of detergents and protein denaturants, pH range variations and high temperature. The analyses conducted with the biotin-avidin system show high precision and the ability to analyse a great number of samples in a short time [41].

The importance of food safety and the detection of pathogenic *L. monocytogenes* in milk

1.4. Food safety

Food choice is increasingly influenced by the psychological interpretation of products' properties, rather than by their actual physical properties [42]. In particular, the perception of food safety and risks is an interpretation that conditions the purchase of a certain food product, thus having consequences for both the consumer and the producer welfare [43]. Consumers reduce their confidence in healthiness of food products mainly because of bacterial outbreaks. An important factor in food safety is thereby the recognition of pathogenic bacteria. This was - and is still - a matter of debate involving policy makers, industries, researchers and the wider public as well [44], since only in the United States, each year from 6 to 81 million diseases are transmitted through food causing more than 9000 deaths [45].

In recent years, new standards regarding hygiene good practices to be carried out in the home setting have been commonly adopted by population and food industry, and new major regulations requiring the use of Hazard Analysis Critical Control Point (HACCP) methods [46] have been implemented, together with advanced biochemical analyses for pathogens bacterial control. In 2009, the Foodborne Diseases Active Surveillance Network (FoodNet) of the Center for

Disease Control and Prevention highlighted a substantial decline of the reported incidence of infections caused by *Campylobacter*, *Listeria*, *Salmonella*, *Shiga* toxin-producing *Escherichia coli* O157, *Shigella* and *Yersinia* [47]. However, many of the foodborne illnesses are sporadic and may not being easily included in outbreaks. The Department of Health and Human Services of the United States has thus launched in 2010 the “Healthy People2010” initiative, with the aim to improve food safety in the United States and to help reduce the incidence of foodborne diseases caused by *Campylobacter*, *E. coli* O157:H7, *Listeria* and *Salmonella*.

1.5. *Listeria monocytogenes* and listeriosis

1.5.1. Discover of *L. monocytogenes*

Listeria monocytogenes was officially described for the first time in 1926 by Murray, who named it *Bacterium monocytogenes* as a consequence of a characteristic monocitosis found in infected rabbits and guinea pigs [48]. There are many reports dating back to 1891 that seem describing *L. monocytogenes* [49]. The authors of these reports, however, did not register the bacteria they isolated in a permanent collection, and this prevented any possibility of subsequent comparisons. In 1927 Pirie and his research group, during investigations performed after some suspicious deaths observed in gerbils near Johannesburg in South Africa, discovered a bacterium similar to that identified by Murray, naming it *Listerella hepatolytica*. The director of the National Type Collection at the Lister Institute in

London decided thus to put Murray and Pirie into contact in order to permit them to compare their findings [50], as the two species of bacteria showed many interesting similarities. Once the perfect overlap between the two microorganisms was finally established, the new bacterium was named with the generic name *Listerella* in honour of Lord Joseph Lister (a British surgeon who distinguished himself for his knowledge in the field of bacteriology) [51], and the specific name *monocytogenes*. The generic name *Bacterium*, suggested by Murray, was rejected because the bacterium did not possess the characteristics of that genus. In 1939 the Judicial Commission on Bacteriological Nomenclature and Taxonomy rejected the generic name *Listerella*, because this name has already been applied by Jahn in 1906 to a group of molds [49], thus in 1940 Pirie proposed the alternative name of *Listeria monocytogenes*, which became the definitive one [50].

1.5.2. Molecular and taxonomical profile of *L. monocytogenes*

L. monocytogenes is an aerobic (and facultative anaerobic), non-sporulating, non-capsulated and Gram-positive bacillus (**Fig. 1.11.**). It is catalase positive and oxidase negative and expresses β -hemolysin. The organism possesses a characteristic tumbling motility, given by his peritrichous flagella (**Fig. 1.12.**), occurring in a narrow temperature range: the movement is expressed mainly at 20-25°C, temperature at that flagellin is both produced and assembled at the cell surface, whilst at 37°C flagellin production is reduced and the flagella are immobile [48].

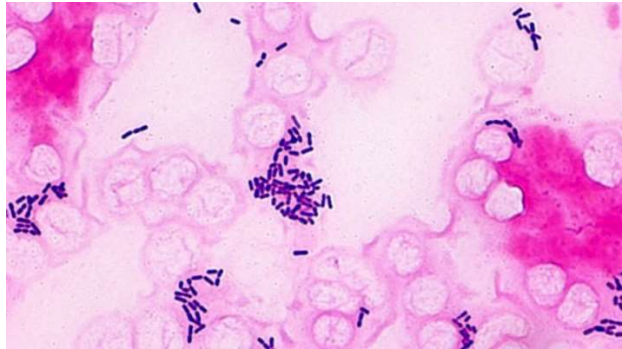


Fig. 1.11. Gram staining highlights *L. monocytogenes* in violet (<http://microbe-canvas.com>).

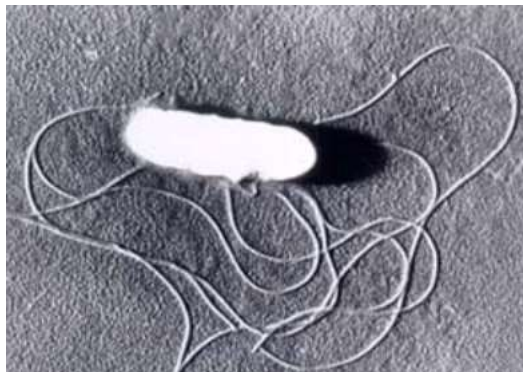


Fig. 1.12. *L. monocytogenes* with its flagella [52].

L. monocytogenes grows in a very wide range of temperature (from 0°C to 45°C) and pH (from 6.0 to 9.0) [53], and it requires a thermal treatment at 72°C for at least 15 seconds to be sensitive to pasteurization. It is able to reduce the

antimicrobial effect of bile salts flowing from the liver to the intestine, thanks to two different systems called BSH (Bile Salt Hydrolase) and BilE (Bile Exclusion System) [54]. This property allows it to survive in the gastrointestinal tract. *L. monocytogenes* is therefore considered an “evolving pathogen”, as a consequence of its adaptability to unfavourable environmental conditions and to the development of an effective antibiotic-resistance system.

For several years, only the species *monocytogenes* belonged to the genus *Listeria* [50], but thanks to the introduction of novel biomolecular methods it was possible to distinguish ten different species, among which a close phylogenetic relationship exists (**Fig. 1.13.**): *L. monocytogenes*, *L. fleischmannii*, *L. grayi*, *L. innocua*, *L. ivanovii*, *L. marthii*, *L. rocourtia*, *L. seeligeri*, *L. weihenstephanensis* and *L. welshimeri* [53].

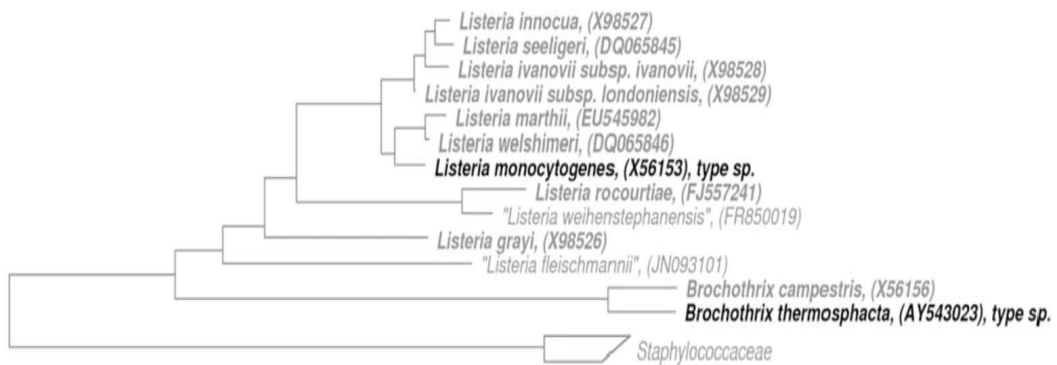


Fig. 1.13.: Phylogenetic tree of *Listeria* genus based on 16S rDNA [53].

After several analyses, it was possible to observe a well conserved genome organization of *Listeria* species and a high number of orthologous genes, but also it emerged that exist characteristic tracts own of each strain [55]. This is a clear indicator that, during the evolutive process, bacteriophages and plasmids played an important role for gene-acquisition [56]. Thanks to the results of many tests *in vitro*, it was possible to characterize the *Listeria* species according to the different combination of somatic antigen (O) and flagellar antigen (H), and to classify them into 15 different serotypes (called serovars), 13 of which are included in *L. monocytogenes* (1/2a, 1/2b, 1/2c, 3a, 3b, 3c, 4a, 4ab, 4b, 4c, 4d, 4e and 7). There are distinct differences in cell surface proteins amongst the different lineages which are independent of the antigens used in serotyping [57]. Using the hybridization DNA/DNA technique, over 90 strains of *L. monocytogenes* have been grouped into three evolutive groups, called “Lineages”, correlated with the different *serovars*. “Lineage I” is in turn divided into two groups: the first includes *serovars* 1/2a and 3a, whilst the second includes *serovars* 1/2c and 3c. “Lineage II” is divided into two groups, the first including *serovars* 4b, 4d, 4e and the second including *serovars* 1/2b, 3b and 7. Finally, “Lineage III” is divided in “Lineage IIIa” including *serovar* 4a, and “Lineage IIIb” including *serovar* 4c [50]. The virulence of the pathogenic *L. monocytogenes* is associated with the synthesis of several proteins, which permit the invasion of the mammalian cells, the escape from phagocytic vacuole, the actin-based motility and the cell-to-cell spread. IlnA and IlnB allow its entry in mammalian cells, while hemolysin O (LLO) and phospholipase C (PI-PLC) permit the escape from vacuoles [58]. Its expression is maximal at 37°C and it is inhibited at 30°C. These trends are directly correlated with the synthesis of the transcriptional factor PrfA, which permits the activation of the bacterial virulence

genes [59] [60]. Intracellular movements require the expression of ActA and the two membranes vacuole is lysed by LLO and a lecithinase (PC-PLC) [58].

1.5.3. Listeriosis

Listeria monocytogenes can cause listeriosis, which is a severe disease with high hospitalization and a case-fatality rates of up to 30% [45]. Both outbreaks and sporadic cases are associated with contamination of various types of food, such as milk, soft cheese, meat, vegetables and seafood products. The ubiquitous nature of the bacterium and its incubation period varying from 1 to 90 days, make the identification of the pathogen in the contaminated food quite difficult.

After the ingestion of contaminated food, it spreads from the intestinal lumen to the central nervous system [56, 61] (Fig. 1.14).

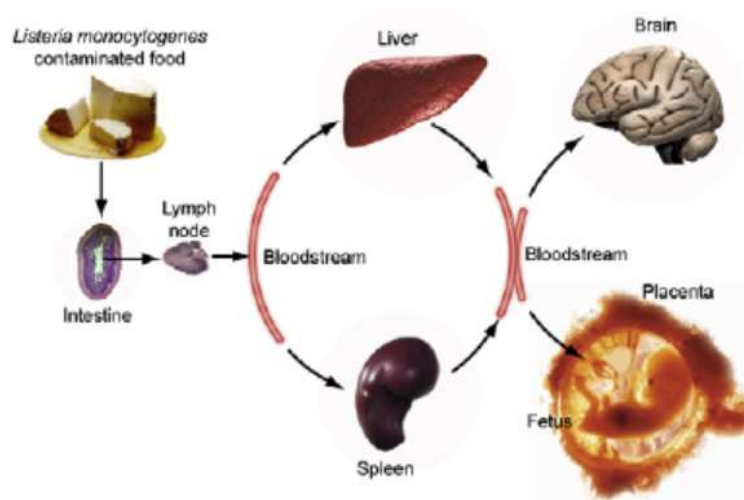


Fig. 1.14. Successive steps of human listeriosis [61].

The pathogen enters into the cells by phagocytosis, it is released from the membrane-bound vacuole and then it begins to multiply [62]. Moving through intracellular actin-based or cell-to-cell, the pathogen infects a vast range of host tissues, with liver as the main site of infection [63]. In the liver, the Küpffer cells kill the majority of the bacteria, inducing apoptosis with concomitant release of chemoattractants, which leads to an influx of neutrophils [64]. These phagocytic cells ingest bacteria or apoptotic hepatocytes. It is a critical step in order to avoid bacterial multiplication and to contribute to the rapid clearing of the infection [65] (**Fig. 1.15.**). Commonly, listeriosis can cause meningitis, septicaemia and other infections involving the central nervous system. It is particularly dangerous for immunocompromised population, such as people undergoing renal transplantation and those with acquired immunodeficiency syndrome (AIDS) and cancer. The risk of listeriosis is indeed estimated to be 100 to 300 times higher in patient with AIDS than in the general population [62]. In pregnant women listeriosis may lead to spontaneous abortion, still birth or fetal death [63].

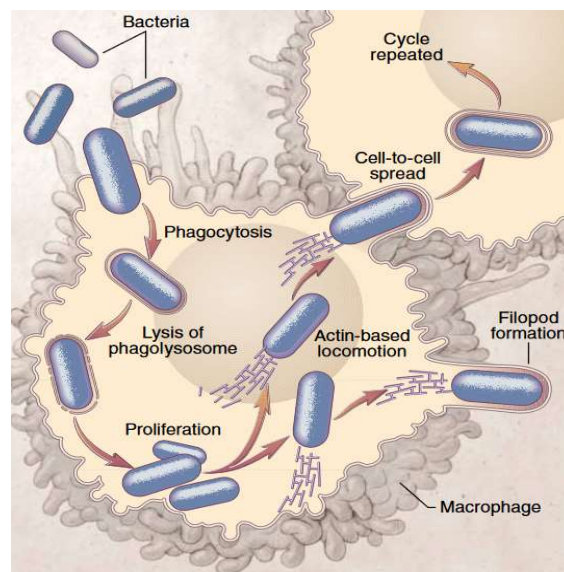


Fig. 1.15. Life cycle of *L. monocytogenes* in host cells [62].

1.6. Classical methods for *L. monocytogenes* detection and enumeration

1.6.1. Qualitative and quantitative methods for detecting *L. monocytogenes*

The minimum infective dose of *L. monocytogenes* has not been established yet. However, the food laws of many countries require that *L. monocytogenes* must be absent in samples of 25 g of ready-to-eat food products [66]. The success of basic protocols for the pathogen detection depends on the number and the state of microorganisms in the sample, the selectivity of media, the conditions of incubation and the electivity of the isolation medium. The EN/ISO 11290-1 describes the method used to isolate *L. monocytogenes* from food samples, following the sequence of pre-enrichment, selective enrichment and isolation on selective media [67]:

- 1) Pre-enrichment, using *Half Fraser Broth*, which is a primary selective enrichment broth;
- 2) Selective enrichment, using *Fraser Broth*, which is a secondary selective enrichment broth;
- 3) Isolation on selective media, taking place on two different media, PALCAM and ALOA.

In the qualitative method, both primary and secondary selective enrichment broths are functional for recovering any stressed bacterial cell.

PALCAM selectivity is due to the presence of selective agents, such as lithium chloride, polymyxin B-sulfate, ceftazidime and acriflavine, which suppress

the growth of many not-*Listeria spp.* bacteria [68]. The medium differentiation is based on aesculin hydrolysis and mannitol fermentation. Indeed, all the *Listera spp.* cause the aesculin hydrolysis, showing blackening of the medium, due to the reaction of ferric ions with the aesculetin, namely the product of aesculin hydrolysis [69]. The presence of the pH indicator phenol red distinguishes mannitol fermenting strains of *Listeria spp.*, by the change of medium colour from red to yellow.

ALOA selectivity is due to the presence of lithium chloride, ceftazidime, polymyxin B-sulfate, nalidixic acid and cycloheximide. The specific medium differentiation is obtained with a specific substrate for phospholipase C, owned only by the pathogenic *L. monocytogenes*. After the isolation, the method expects that at least five hypothetical colonies of *L. monocytogenes* are selected in order to confirm their identities through several tests (such as haemolysis test, CAMP test and other biochemical tests).

The quantitative method (referring to the consolidate version of the Commission regulation 2073/2005, the method is described by the EN/ISO 11290-2) is based on the above mentioned analyses referring to the EN/ISO 11290-1, but, in addition to them, in this case characteristic *L. monocytogenes* colonies are enumerated [70].

These standard procedures may take four/five days to obtain a negative result and two/three days for a hypothetical positive one and its confirmation. However, often this timing is not compatible with the market, due to food perishability and the need to protect consumers.

1.6.2. Molecular methods for detecting *L. monocytogenes*

One of the most frequently used molecular methods for *L. monocytogenes* detection is the real-time PCR (*Polymerase Chain Reaction*), based on the standard legislation ISO 16140. A standard document provides requirements, specifications, guidelines, or characteristics that can be used consistently to ensure that materials, products, processes and services are fit for their purpose.

This method is one of the most innovative and widely used in the field of life science, as it can give rapid results one day after the analysis [71]. It is composed by different, subsequent stages [72]: **a)** matrix enrichment, **b)** nucleic acids extraction and purification, **c)** target amplification using specific primers, and **d)** PCR products determination.

This method is based on one or two enrichment phases, coupling one bacterial-DNA extraction and one real-time PCR assay. It permits to quantify the microorganisms in the sample and to measure step-by-step the fluorescence generated during the polymerase chain reaction, thanks to two different detection systems of PCR-products accumulation: dyes linked to DNA double strands, and probes linked to fluorescent molecules. Compared with the qualitative and quantitative methods previously described (EN/ISO 11290-1 and 11290-2), this one appears to be more reliable [73], thanks to its higher performances, accuracy, specificity, sensitivity and its shorter running time.

1.6.3. Immunological methods for detecting *L. monocytogenes*

Every immunological assay is based on the optimal combination between the specificity of antigen-antibody and the detection sensitivity of a tracer, which changes for each assay in order to take advantage of the specific interaction antigen-antibody.

In 1980s, numerous studies investigated the immunodetection of DNA. As a result, the polymerase chain reaction-enzyme linked immunosorbent assay (PCR-ELISA) was introduced [74]. PCR-ELISA is an analytical technique that allows to quantify the PCR product directly after immobilization of biotinylated DNA on a microplate. This method involves three steps [75]: 1) amplifying the gene of interest by PCR technique, 2) binding PCR products with the specific gene of interest to the microplate, using biotin-avidin complex, whilst all non-specific products are washed off, and 3) detecting biotinylated DNA, made visible and measurable by the use of a spectrophotometer.

This is the more reliable mass-screening method to detect and screen *Listeria spp.* in food. The presumptive positive results offered by ELISA have to be confirmed by a PCR-based method [76]. PCR-ELISA is a sensitive tool with many advantages. First, it allows detection at very small concentrations; second, it can be carried out using standard laboratories; and third, it is more cost-effective than real-time PCR [74].

Commercially available immunological methods for *Listeria* identification are numerous, such as VIDAS (BioMérieux, France), *Listeria* Tek (Organon Teknika, USA), *Listeria* VIP (BioControl, USA), *Listertest* (Vicam, USA) and *Pathatrix* (MatixMicroscience, UK).

1.7. Innovative methods for *L. monocytogenes* determination

1.7.1. Micro-gravimetric biosensor

Micro-gravimetric biosensor is an immunosensor composed of peculiar materials, which displays piezoelectric properties. The term “piezoelectric” derives from the Greek word *piezen*, meaning “to press” and when the electrical field changes, the application of a potential difference induces a compression (or an expansion) of the material. This is the “piezoelectric effect”, namely a reversible effect that corresponds to an internal mechanical stress, induced by an applied potential. The system used is a quartz crystal resonator, composed of a quartz disk with a thin gold film on both sides [77]. Quartz is a natural material, specifically cut for maintaining the symmetry of the crystal (this is a basic property for this application). If a potential with a certain periodicity is applied, the piezoelectric properties allow creating acoustic waves, which are propagated perpendicularly on the quartz crystal surface [78]. The contact of quartz with a liquid solution can modify the oscillation, causing interactions between charges or dipoles in the fluid, as well as superficial charges of the material. This phenomenon can interfere with the normal propagation of acoustic waves, causing the “electroacoustic effect”. If the quartz is coated with a conductor material such as gold, this effect could be avoided. In 1980, Konash showed that a quartz crystal resonator, immersed in a liquid phase, could oscillate [79].

The main advantage of this method is due to the ability of quartz crystal resonator to operate in fluids. One of the main purposes of biosensing is indeed the successful characterization of biomolecular systems in their natural

environment, namely water [80]. The main applications of the method are based on weighing the mass deposited or removed from the crystal surface. The quartz crystal has indeed a basic frequency depending on its geometry, which linearly decreases with the mass deposited on the surface, according to Sauerbrey equation:

$$\Delta f = - \frac{2f_0^2}{A\sqrt{\rho_q\mu_q}} \Delta m$$

Δf : frequency change (Hz)

f_0 : resonance frequency of crystal (Hz)

A : piezoelectric area (cm²)

ρ_q : quartz density (2.648 gcm⁻³)

μ_q : shear module of quartz (2.947x10¹¹ g/cms²)

Δm : mass change on the quartz surface (g)

In addition, information can be obtained from the material on the surface of resonator, recording the energy loss during the oscillation [81].

A micro-gravimetric biosensor is characterized by high sensitivity, label or radiation free entities and low cost. These properties allow to investigate biomolecular interactions and clinical bioassays [82].

Several methods have been developed in order to immobilize antibodies onto the piezoelectric quartz crystal. In particular, the application of self-assembled monolayers, coupled with magnetic nanoparticles, increases the amount of

immobilized biomolecules and provides numerous advantages for sensor performances [83].

1.7.2. Biosensing and magnetic nanoparticles

Biosensing is based on immobilized biomolecules for the determination and detection of target analytes. These sensing biomolecules should be immobilized on the surface of a signal transducer, and the subsequent biological-recognition generates then an optical, electrical or microgravimetric signal [84]. Magnetic nanomaterials are an efficient and powerful exploitable source for biosensing, due to their strong magnetic properties (not present in biological systems), which permit signal amplification, single molecule-detection, and new signal transduction mechanisms [85]. In addition, the development of new portable devices facilitated the use of nanoscale magnetic materials, since lengthy sample purification and long assay times are no longer required [86].

Magnetic nanoparticles are an example of nanomaterials used for biosensing. A nanoparticle may be defined as an entity having three dimensions of the order of 100 nm or less, and its properties are dramatically different from bulk materials [87]. A magnetic nanoparticle generally consists of a magnetic element (iron, oxides, cobalt, nickel) or its chemical oxides. Magnetic nanoparticles, coupled with a bioelement, show high biocompatibility and biochemical stability in physiological conditions. For these reasons, they can be applied for drug delivery, medical imaging and protein purification [88]. The safety of nanoparticles is very important

for their food-related application. They have to present indeed no toxicity, good biocompatibility and they do not have to maintain residual magnetism after the removal of the external magnetic field. The superparamagnetic nanoparticles (Fe_2O_3 and Fe_3O_4) respond to these requirements [89]. Other examples are: **(a)** gold nanoparticles (AuNPs), used to detect streptomycin in blood serum and milk thanks to their high sensitivity, chemical stability, ease of synthesis and the characteristic of being attractive energy acceptors [90]; and **(b)** iron/gold core/shell (Fe@Au) nanoparticles conjugated with anti-*Salmonella* antibodies, used to detect *Salmonella typhimurium* in milk [91].

In the present experimental work, a novel nanomaterial called SAMNs (Surface Active Magnetic Nanoparticles) was used for detecting *L. monocytogenes* in milk. It is composed of stoichiometric maghemite ($\gamma\text{-Fe}_2\text{O}_3$), which presents a characteristic surface chemical behaviour. SAMNs have been developed in the laboratory of Professor Fabio Vianello (Department of Comparative Biomedicine and Food Science, University of Padova), and they are currently protected by international patent (patent number: US 8980218, 2015; EP 2596506B1, 2014). This nanostructured superparamagnetic material has numerous advantages compared with traditional iron oxides, because its synthesis is carried out exclusively in water, avoiding the disposal processes of organic solvents and thus reducing costs [92]. SAMNs, without any superficial modification, are dispersible in water, stable in suspension for several months and can be used to immobilize specific organic molecules [93]. These nanoparticles are superparamagnetic, a property that occurs when a material have casual oriented magnetic dipoles, which can be orderly oriented in presence of an external magnetic field [94]. When the magnetic field is removed, nanoparticles lose their magnetic property and, as a

consequence of the lack of magnetic force (responsible of the aggregation phenomenon), dipoles arrange again in disorderly manner.

Nanoparticles do not show, therefore, magnetic characteristics *per se*, as the latter are displayed only in presence of an external magnetic field, without which nanoparticles do not form aggregates. It is important to note that magnetic nanoparticles can be easily derivatized for immobilizing antibodies, and then they have the capability to amplify and improve the immunosensor signals. The intensity of the final signal will depend on the amount of antigen recognized by the antibody bound on nanoparticle surface.

AIM OF THE PROJECT

CHAPTER 2

The main purpose of the present research work was to develop a new immunosensor for detecting *L. monocytogenes* in milk. This ubiquitous bacterium can cause listeriosis. Listeriosis is a disease particularly dangerous for immunocompromised population, such as people undergoing renal transplantation and those with acquired immunodeficiency syndrome (AIDS) and cancer. In pregnant women, it may lead to spontaneous abortion, and it is associated with contamination of various types of food, such as milk.

The immunosensor proposed for the detection of *L.* consisted of a piezoelectric quartz crystal characterized by a resonance frequency of 9,5 MHz, coated with two gold electrodes on each surface and with the ability to operate in fluids. The quartz crystal had a basic frequency, which linearly decreased with the mass deposited on the surface. The piezoelectric crystal was derivatized with cysteamine, biotin, avidin and antibodies against *Listeria monocytogenes* (Ab-*L. monocytogenes*) and several concentrations of bacteria were tested on the crystal surface. Its ability to detect known concentration of *L. monocytogenes* in milk was explored. In addition, the specificity of the system was tested injecting the known concentration of *L. innocua*.

In order to improve the analytical performances of the immunosensor, a novel procedure was introduced. This novel procedure involved the application of magnetic nanoparticles coated with biotinylated antibodies against *L. monocytogenes*, and leading to the development of a magnetic nanosized complex, SAMN@Av@Ab-*L. monocytogenes*, which was used **a)** to eliminate interfering substances in the milk matrix before the measurements, **b)** to identify and capture *L. monocytogenes* bacteria in milk and **c)** to amplify the signal obtained by the piezoelectric system. In order to support the experiments, a traditional microbiological method (i.e., plate count) was used as control.

Results showed that the proposed system can be proposed for the detection of concentrations of *L. monocytogenes* in milk in short times and with low costs.

MATERIALS AND METHODS

CHAPTER 3

The preparation of bacterial culture and instrumentation to detect *L. monocytogenes* in milk

3.1. Reagents and solvents applied

The substances used for the experiment are reported in the **Tab. 3.1**. The reagents were purchased at the maximum purity obtainable, such as not to require purification treatments before use.

PRODUCT NAME	ABBREVIATION	SUPPLIER
Ab- <i>L. monocytogenes</i> (Biotin) modified		GeneTex
ALOA medium		Biolife Italiana S.r.l.

Avidin		IBA Biotechnology
Biotin		Sigma - Aldrich
Cysteamine hydrochloride		Fluka
Di-Sodium hydrogen phosphate dihydrate		Carlo Erba
Ethanol		Sigma – Aldrich
Magnetic nanoparticles	SAMNs	-
Milk UHT		Parmalat
N-AGAR medium		Biolife Italiana S.r.l.
N-Cyclohexyl-N'-(2-morpholinoethyl) carbodiimide methyl-p-toluenesulfonate	CMC	Sigma – Aldrich
N-hydroxysuccinimide	NHS	Fluka
N, N-Dimethylformamide anhydrous	DMF	Sigma – Aldrich
Phosphate buffer salite	PBS 1X	-

Tetramethylammonium hydroxide	TMAOH 1M	-
Tryptic soy broth	TSB	-
TSAYE medium		Biolife Italiana S.r.l.

Tab 3.1. List of reagents and solvents used in the experiments.

3.2. Preparation of inactivated *L. monocytogenes* inoculums

For the present research, a standardized inoculum of *L. monocytogenes* ATCC 19117 serotype 4d and *L. innocua* ATCC 33090T serotype 6a were prepared by Dr. Luca Fasolato of the Department of Comparative Biomedicine and Food Science, University of Padova. The protocol of inactivation was performed according to Datta et al. [95]. The strains were revitalized at 37°C for 48 h on ALOA medium. A single pure colony was inoculated in 12 mL of TSB (trypticase soy broth) and incubated overnight at 37°C, allowing a final concentration around 8 Log₁₀ (colony forming unit CFU/mL). After centrifugation, broths were washed twice on physiological solution. The optical density (OD₆₀₀) was evaluated by spectrophotometric method (MultiskanGo Thermoscientific), and the enumeration of washed inoculums of *Listeria* were performed by plate count method in plate count agar (PCA; Oxoid) and ALOA. Then, the inoculums were inactivated in a

thermal bath at 73°C for 1 h and stored, after the sterility test, at -80°C for a maximum period of 4 months.

3.3. The piezoelectric system

The system used in this experimental work consists of a piezoelectric quartz crystal (ElbaTech S. r. l.), characterized by a resonance frequency of 9,5 MHz, coated with two gold electrodes on each surface (**Fig. 3.1.**). The crystal is placed in a flow chamber, containing an O-ring, that allows to isolate one of the two surfaces (**Fig. 3.2.**). It permits to use each surface for different analyses and to obtain a stable frequency.



Fig. 3.1. Structure of a piezoelectric quartz crystal with its support.



Fig. 3.2. Flow chamber with the O-ring.

The flow chamber, in which is inserted the quartz crystal, is connected, to a computer controlled injection valve system, and, on the other side, to a frequency oscillator connected with the computer (**Fig. 3.3.**).

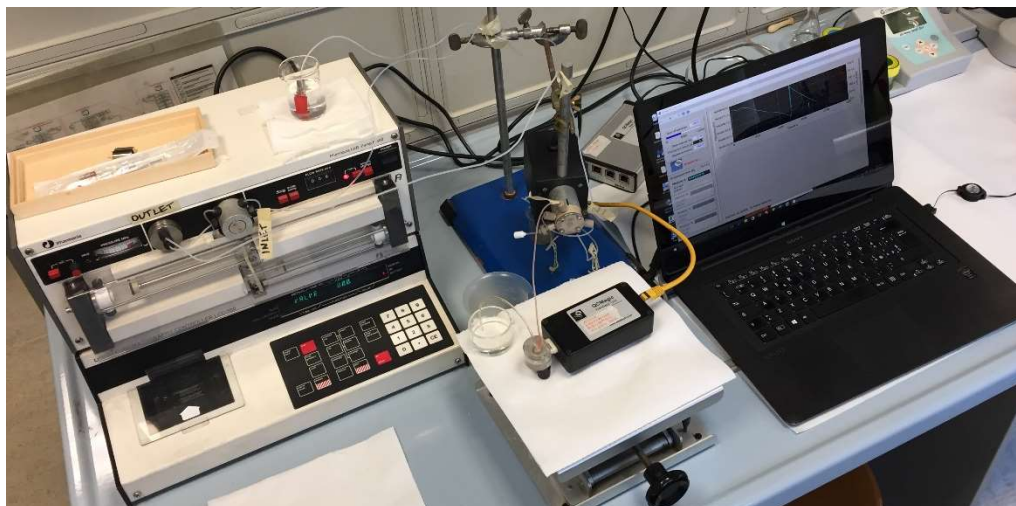


Fig. 3.3. Piezoelectric system.

A computer controlled syringe pump provided the injection of the solvent on the quartz crystal surface (previously derivatized), with a constant flow of 6 mL/h. The following parameters were added to the software registration mode:

- Acquisition number: 10 000 pt. It is necessary to obtain a significant measure.
- Temporal gap: 0,5 seconds. It is the gap between two subsequent measurements.
- Delay between two measurements: 0,5 seconds. It affects the system accuracy.
- Statistic samples: 10. During the acquisition, the software calculates the average and the standard deviation of n samples.

When the acquired signal was stable, the sample was injected into a loop (volume of 100 μ L) in the injection valve and, dragged by the solvents to the crystal surface. *QC Magic R3* recorded a decrease in frequency proportional to the total mass deposited on the crystal surface. Phosphate Buffer Saline (PBS) was used as solvent, because it is optimal for antibody antigen recognition process and guarantees stability of the crystal resonance frequency. In addition, it allows to dilute and hydrate biomolecule, immobilized on the surface. Repeated washings with PBS can cause the complete dissociation of the analyte and an increase is expected in frequency to values, recorded before the sample injection (**Fig. 3.4.**)

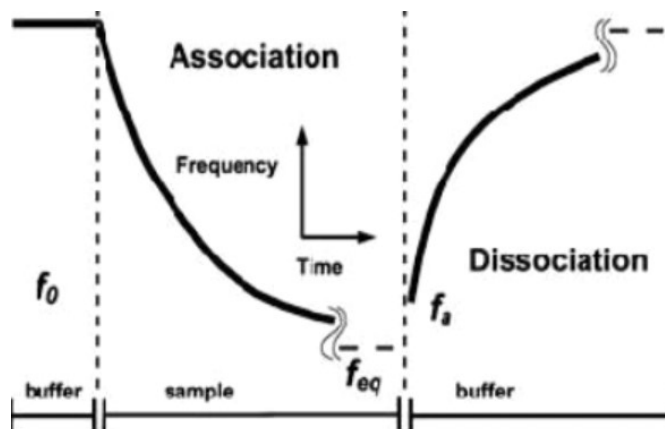


Fig. 3.4. Basic principle of piezoelectric.

3.4. SAMNs

3.4.1. Synthesis of SAMNs

The magnetic nanoparticles were synthesized following the method described by Magro et al. [92]. $\text{FeCl}_3 \cdot 6\text{H}_2\text{O}$ (10.0 g, 37 mmol) was dissolved in Milli-Q water (800 mL) at room temperature and under vigorous stirring. Then, NaBH_4 solution (2 g, 53 mmol) in ammonia (3.5%, 100 mL, 4.86 mol/mol Fe) was added to the mixture. After the reduction reaction, the temperature of the system was increased to 100°C and maintained constant for 2 h under stirring. The material temperature was decreased at room temperature and aged in water for further 12 h. The product obtained was separated by the action of an external magnet for 60 minutes. Then, it was washed with water several times. The material can be transformed into a

red/brown powder by drying and curing at 400°C for 2 h. After thermal treatment were obtained individual nanoparticles. The nano-powder showed a magnetic response, whether it was exposed to a magnetic field. The final mass produced was 2.0 g (12.5 mmol) of Fe₂O₃. A yield of 68% was calculated. The obtained nanomaterial was characterized by zero field and in field (5 T) Mössbauer spectroscopy, FTIR spectroscopy, high resolution transmission electron microscopy, XPRD and magnetization measurements. It was constituted of stoichiometric maghemite (γ -Fe₂O₃) with a mean diameter of 11±2 nm. It can lead to the formation, after sonication in water (Bransonic, model 221.48 kHz, 50 W) of a stable colloidal suspension, without any organic or inorganic coverage. These bare maghemite nanoparticles were called “Surface Active Maghemite Nanoparticles” (SAMNs).

3.4.2. Derivatization of SAMNs with avidin and Ab-*L. monocytogenes*

SAMNs can be reversibility derivatized with selected organic molecules. In this research, they were superficially derivatized by simple incubation in water solution in the presence of avidin. Bare SAMNs (50 mg/L) was incubated with 100 mg/L avidin in 50 mM TMAOH pH 7.0 at 4°C, in the dark, overnight and with continuous agitation. TMAOH guarantees higher stability of the nanoparticles than water as they remain stable in suspension. After incubation, the nanoparticles were removed with an external magnet and the amount of bound avidin was calculated from the disappearance of the absorbance at 280 nm in the supernatants ($\epsilon_{280\text{nm}} = 6.99 \times 10^4 \text{ M}^{-1} \text{ cm}^{-1}$) with the spectrophotometer *Agilent Technologies Cary 60*.

Alternatively, bound avidin was evaluated by spectrometry after their release from nanoparticles by treatment with 0.5 M ammonia. SAMN@avidin complexed were magnetically isolated. Subsequently, SAMN@avidin were washed with 50 mM TMAOH pH 7.0 and then with Milli-Q water and finally stored with Milli-Q water.

In this work, a specific antibody for *L. monocytogenes* modified with biotin was used bound to nanoparticles. SAMN@avidin were incubated in a solution with PBS and biotinylated Ab-*L. monocytogenes* of GeneTex at 4°C, in the dark overnight with continuous agitation. Immediately before their use, the SAMN@Av@Ab-*L. monocytogenes* were magnetically separated and the solvent with unbound antibody was replaced with fresh PBS.

3.5. Tests for *L. monocytogenes* capture

3.5.1. Citotoxicity test to evaluate the effects of SAMNs on *L. monocytogenes*

Different concentrations of bare SAMNs were inoculated in *L. monocytogenes* cultures to observe their possible toxicity effect in different incubation times. Three different final concentrations of SAMNs in PBS were used in a final volume of 2 mL: 20 mg/L, 50 mg/L and 100 mg/L. The *L. monocytogenes* strain ATCC 19117, stored at -80°C, was incubated twice (A and B replicates) on ALOA medium at 37°C for at least 24 h. A single pure colony of both replicates was inoculated in TSB at 37°C for 21 h. The next day, immediately before the start

of the experiment, the serial dilutions from 10^8 to 10^3 concentration of *L. monocytogenes* were performed in PBS solution. The 10^3 concentrated samples were used as starter samples for the experiments, because previous studies indicated this concentration of *L. monocytogenes* as optimal. The toxicity tests were performed at 4 different experimental times (t_0 , after 1 h t_1 , after 4 h t_4 , and after 6 h t_6) in order to evaluate the decrease of *Listeria* concentrations.

In order to evaluate the CFU reduction, the samples were inoculated as control both in ALOA and N-AGAR medium at 37°C for 24 h. Samples of the three SAMNs concentrations were incubated only in N-AGAR at 30°C for 24 h, to exclude the presence of contaminants. Then SAMNs were incubated with the starter samples of *L. monocytogenes* (10^3) and three subsequent dilutions were performed.

The \log_{10} CFU/mL of each tests were modelled with the DMFit program in order to define the regression curves of each treatment [96].

3.5.2. *L. monocytogenes* capture experiments with bare SAMNs and SAMN@Av@Ab-*L. monocytogenes* in PBS

Several experiments were performed in order to evaluate the capture of *L. monocytogenes* from PBS and from real matrices such as milk. The results were expressed in UFC/mL, and were obtained applying the following formula for bacterial colonies' count:

$$N = \frac{\Sigma \text{ colonies}}{V(n_1 + 0,1 \cdot n_2)d}$$

N = numbers of units forming colonies

Σ colonies = sum of colonies

V = volume of inoculum

n₁ and n₂ = number of considered plates

d = dilution factor for the first dilution considered

This formula was applied on dilutions in which the values of the plate count were between 10 and 300 colonies. Capture efficiency (CE) [97] was previously evaluated on PBS considering the concentration of 100 mg/L of bare SAMNs and the same concentration of SAMN@Av@Ab-*L. monocytogenes*. The total number of bacteria collected by SAMN@Av@Ab-*L. monocytogenes* can be expressed as pellet or supernatant percentages. These describe the magnetic separation efficacy on *L. monocytogenes* recovered. The supernatant index was useful to calculate the percentage of capture efficiency (CE) [97]:

$$CE = 1 - \left(\frac{C_b}{C_0} \right) \times 100$$

CE = capture efficiency

C_b = number of cells in supernatant

C₀ = total number of cells in the sample

The CE can be calculated using the value of pellet percentage [98]:

$$CE = \left(\frac{C_0}{C_b} \right) \times 100$$

CE = capture efficiency

C_0 = total number of cells in the sample

C_b = number of cells in pellet

Taken together, the supernatant and pellet percentages were useful to calculate the percentage of not recovered cells (NR) in the samples:

$$NR = \frac{n^\circ \text{ total cells} - (n^\circ \text{ pellet cells} + n^\circ \text{ supernatant cells})}{n^\circ \text{ total cells}} \times 100$$

Four different concentration of *L. monocytogenes* strain ATCC 19117 were applied (CFU: 10^4 , 10^3 , 10^2 , 10^1). The modality of inoculum preparation was the same as describe before for the toxicity tests.

Briefly, a single pure colony of both experimental duplicates was inoculated in TSB at 37°C for 21 h. The next day, immediately before the start of the experiment, the serial dilutions from 10^8 to 10^1 concentration of *L. monocytogenes* were performed in solution PBS. Samples of bare SAMNs and SAMN@Av@Ab-*L. monocytogenes* were incubated only in TSAYE medium at 37°C for 24 h, to exclude the presence of contaminants. Then, SAMNs and SAMN@Av@Ab-*L. monocytogenes* were incubated with the different concentration (10^4 , 10^3 , 10^2) of *L. monocytogenes* in a final volume of 2 mL and, immediately after, their three subsequent dilutions were performed. These samples were plated both in ALOA and TSAYE medium at 37°C for 24 h. The rest of the samples were left incubating

for 40 minutes, and then a magnetic separation with an external magnet was performed for 30 minutes. After that, supernatants with their three subsequent dilutions were plated both in ALOA and TSAYE at 37°C for 24 h. Pellets were re-suspended in an equal volume of PBS and were spread both in ALOA and TSAYE at 37°C for 24 h (**Fig. 3.5.**).

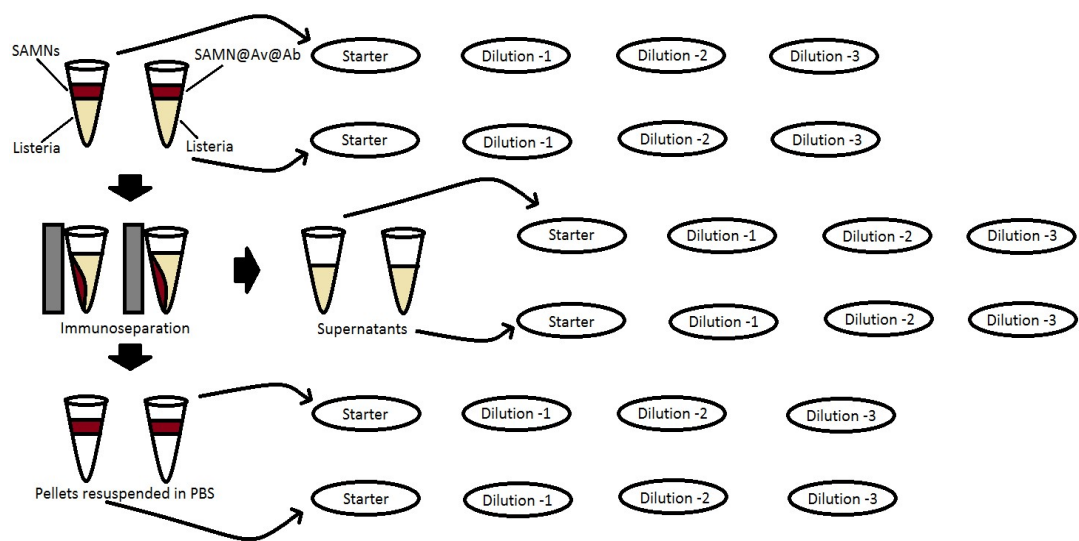


Fig. 3.5. Immunoseparation diagram.

Finally, Eppendorf containing pellets were washed with PBS and then plated for the subsequent enumeration with their three subsequent dilutions both in ALOA and TSAYE at 37°C for 24 h, in order to observe whether bacterial cells remain linked to the plastic tube.

The lower concentrations of *L. monocytogenes* (10^1 and 10^2) were incubated in the presence of 100 mg/L SAMN@Av@Ab-*L. monocytogenes* in PBS, to

observe whether a proportional correlation exists with the results obtained in the previous experiments with higher concentration of *L. monocytogenes*.

3.5.3. Capture test with different concentration of SAMN@Av@Ab-*L. monocytogenes* in PBS and in milk

Two concentrations of SAMN@Av@Ab-*L. monocytogenes* (100 mg/L, 200 mg/L) were inoculated in *L. monocytogenes* cultures to observe their ability to capture *L. monocytogenes* both in PBS and in milk. The *L. monocytogenes* strain ATCC 19117, stored at -80°C, was incubated twice (A and B duplicates) on ALOA medium at 37°C for at least 24 h. A single pure colony of duplicates of each experiment were inoculated in TSB at 37°C for 21 h. The next day, immediately before the start of the experiment, the serial dilutions from 10⁸ to 10³ concentration of *L. monocytogenes* were performed in solution PBS. For the experiment conducted in milk, the last concentration, 10³, was performed in milk. Samples of the three concentration of SAMN@Av@Ab-*L. monocytogenes* were incubated only in TSAYE medium at 37°C for 24 h, to exclude the presence of contaminants. The 10³ concentrated samples were used as starter samples for the experiment. Then, the three concentrations of SAMN@Av@Ab-*L. monocytogenes* were incubated with the starter samples of *L. monocytogenes* (10³) and, immediately after, their three subsequent dilutions were performed. These samples were incubated both in ALOA and TSAYE medium at 37°C for 24 h. The rest of the samples were left incubating for 30 minutes and then a magnetic separation was performed with an external magnet for 15 minutes. After that, supernatants with

their three subsequent dilutions were incubated both in ALOA and TSAYE at 37°C for 24 h. Pellets were re-suspended in an equal volume of PBS and were incubated with their three subsequent dilutions both in ALOA and TSBYE at 37°C for 24 h.

The CE% values were submitted to the arcsine transformation. The data were analysed by the student's t-test in order to evaluate statistical differences among treatments and culture mediums applied in the experiments. These analyses were performed using the IBM ® SPSS ® Statistics 20 Core System.

RESULTS AND DISCUSSION

CHAPTER 4

Effectiveness of the new immunosensor in detecting *L. monocytogenes*

4.1. Antibody immobilization on piezoelectric quartz crystal and response to mass addition of *L. monocytogenes*

4.1.1. Derivatization of crystal surface and the qualitative method to detect *L. monocytogenes*

In this present research work, the piezoelectric quartz crystal was used to develop an immunosensor, exploiting the high affinity of the avidin-biotin system. Several concentrations of inactivated *L. monocytogenes* in PBS (from 10^1 to 10^5 CFU/mL) were injected in the flow cell containing the quartz crystal not-modified, and no change in frequency was recorded. The results have been processed by the *Sigma Plot* software, in which the bacteria detection is expressed as a function of relation to the acquisition time (s) on the abscissas axis, and to the frequency (Hz) on the ordinate axis. The constant value of the frequency of the crystal highlighted

that the bare gold surface of crystal did not bind *L. monocytogenes*. The next step was to immobilize the biotinylated antibody on the quartz crystal surface for observing its response in the presence of *L. monocytogenes*.

This is a new system of antibody immobilization on the piezoelectric biosensors, in literature different approaches are described [99, 100]. For this reason, a detailed description of the experiments was reported in the results section.

Before the measurement, the gold surface of the quartz crystal was derivatized, exploiting the biotin-avidin system. The crystal was cleaned with 99.8% ethanol at room temperature, in the dark, for 30 minutes. In order to immobilize biotin, preliminary, the crystal was submerged in a solution of 50 mM cysteamine hydrochloride and 99.8% ethanol, at room temperature, in the dark overnight (**Fig. 4.1.**) leading to a SAM of cysteamine on gold, as described in Chapter 3.



Fig. 4.1. Binding between cysteamine and the gold surface of the crystal.

The subsequent day, the crystal was washed with 99.8% ethanol to remove the excess of the thiol and it was incubated in the presence of 10 mM biotin, 50 mM NHS and 50 mM CMC in anhydrous DMF at 4°C, in the dark overnight (**Fig. 4.2.**)

in order to provide the condensation of biotin in the solvent exposed $-NH_2$ groups of immobilized cysteamine.

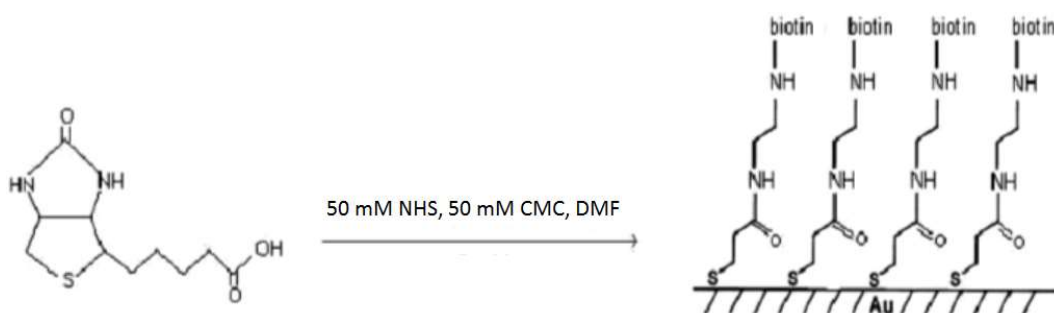


Fig. 4.2. Binding between biotin and the gold surface of the crystal.

After biotin incubation, the crystal was washed with anhydrous DMF in order to remove the excess of reactants, and it was immersed into avidin solution in PBS (1 mg/mL) at room temperature, in the dark overnight. The modified surface was washed with PBS at room temperature, in the dark for 30 minutes, and then the biotin labelled polyclonal antibodies against *L. monocytogenes* was immobilized with PBS on the surfaces of the crystal, with a final concentration 100 $\mu\text{g/mL}$ at 4°C, in the dark overnight. Finally, the antibody-coated crystal was washed with PBS to remove the excess unbound antibody and was stored at 4°C until use.

The crystal was inserted in the flow cell and several concentrations of *L. monocytogenes* (from 10^1 to 10^5 CFU/mL) without SAMNs were injected into the piezoelectric system in ascending order. The immunosensor response, for each injection, was achieved within 5-10 minutes from the introduction of bacteria into

the flow loop. Changes in the crystal frequency were recorded, due to the mass variation on the crystal surface. This indicated the bacteria recognition and their capture by the immobilized antibody on the crystal surface. The results have been processed by the *Sigma Plot* software. The biotinylated Ab-*L. monocytogenes* captured the bacterium from the lowest concentration of 10^1 CFU/mL to 10^5 CFU/mL, showing a gradual frequency decrease for each bacterial concentration injected (**Fig. 4.3**). The determination of the frequency variation (ΔF) of the modified crystal allowed to build a calibration curve, related to the amount of bacteria injected into the system, with a correlation coefficient of 0.99 (**Fig 4.4**). The frequency decreased proportionally with the bacterial concentrations. Therefore, the value of each ΔF - corresponding to a higher bacterial concentration - must be higher than the initial ΔF : a shift of 20 ΔF (Hz) was obtained after the introduction of *L. monocytogenes* at 10^1 CFU/mL and the injection of *L. monocytogenes* at 10^4 CFU/mL decreased further the frequency of 60 ΔF .

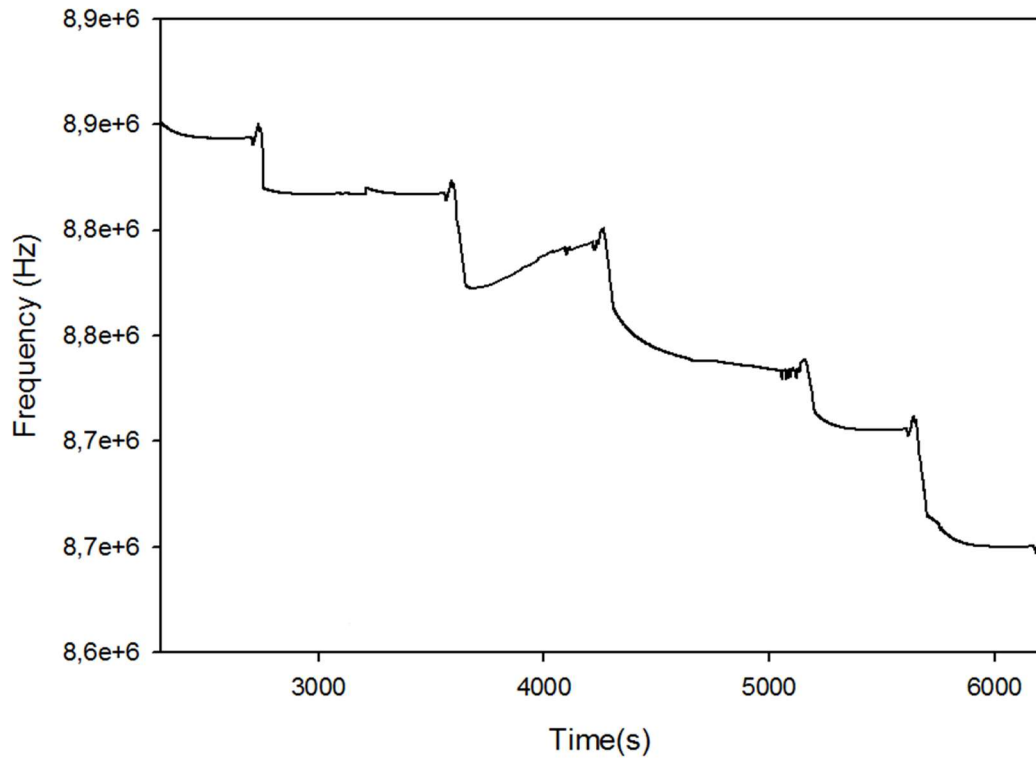


Fig. 4.3. The immunosensor run.

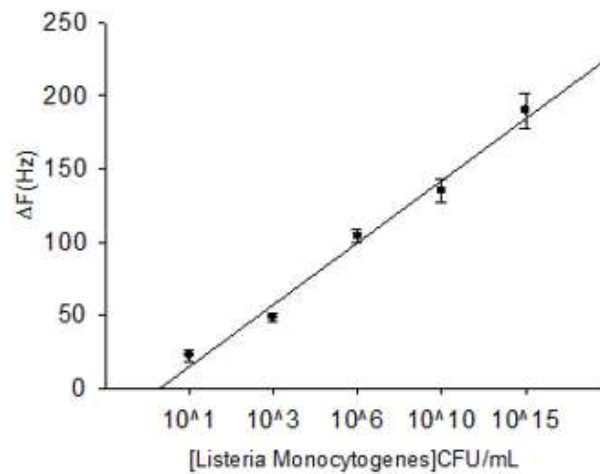


Fig. 4.4. The calibration curve related to the amount of bacteria injected into the system.

The calibration curve allowed to obtain the sensitivity and the limit of detection (LOD) of the immunosensor. It detected and quantified *L. monocytogenes* with a LOD of 3 cells/200 μ L and with a frequency change of about 2 Hz (**Fig 4.5.**). This result was significantly better than other piezoelectric detection of *L. monocytogenes* in milk reported in the literature with a LOD of 10^3 CFU/mL [101].

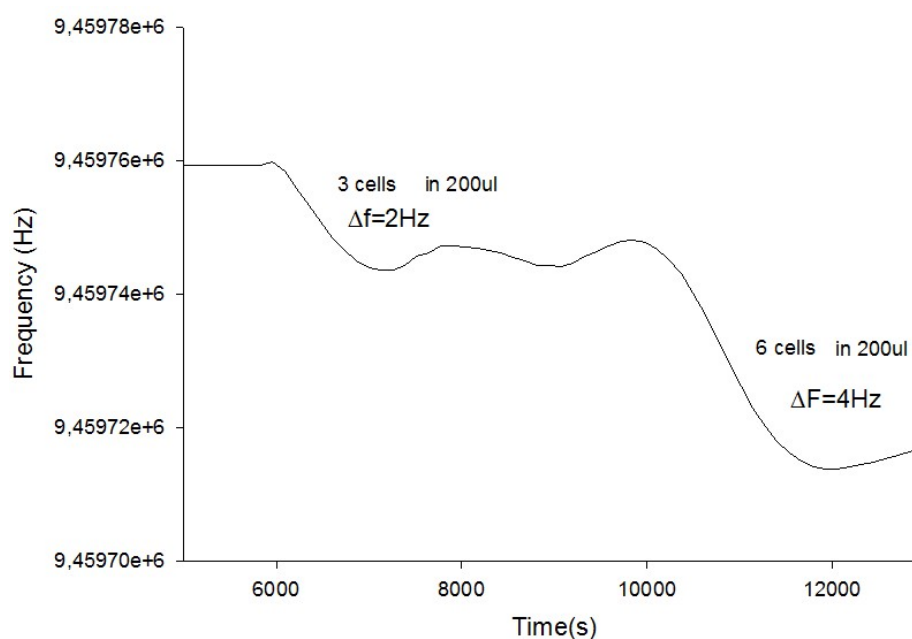


Fig. 4.5. Limit of detection of *L. monocytogenes* with the piezoelectric quartz crystal.

4.1.2. Amplification of piezoelectric signal of *L. monocytogenes* by the SAMN@Av@Ab-*L. monocytogenes*

The piezoelectric quartz crystal can be used for carrying out both qualitative analyses, based on the mass variation on the surface of piezoelectric quartz crystal, and quantitative ones, by estimating the bacterial concentration at a given frequency. The use of coated nanoparticles with Ab-*L. monocytogenes* has been suggested with the aim to create a new generation of amplification systems for immunosensors. The creation of the sensing layer, using a biotinylated antibody, permits to control the orientation of the antibody on gold surfaces, preserving its bioactivity and increasing the affinity for *L. monocytogenes*. In this research, it was developed a method to capture inactivated *L. monocytogenes* in solution (first in PBS and then in milk) with SAMN@Av@Ab-*L. monocytogenes* and then to detect this complex with the piezoelectric quartz crystal.

First, SAMNs were derivatized with avidin, as described in Paragraph 3.4.2. The solution composed by 100 mg/L avidin in 50 mM TMAOH was observed with the spectrophotometer *Agilent Technologies Cary 60*, and the characteristic absorbance peak of avidin was identified at 280 nm. The solution containing SAMNs was then incubated. After a magnetic separation, the supernatants were observed with the spectrophotometer. The reduction of avidin peak at 280 nm confirmed the binding between SAMNs and avidin. Subsequently, one wash with TMAOH and one with Milli-Q water were performed in order to remove the unbound avidin. Each washing was observed by the spectrophotometer (**Fig. 4.6.**). It was very important to verify the actual creation of a link between SAMNs and

avidin, as it is a prerequisite for the subsequent creation of a binding between SAMN@avidin and the biotinylated antibody.

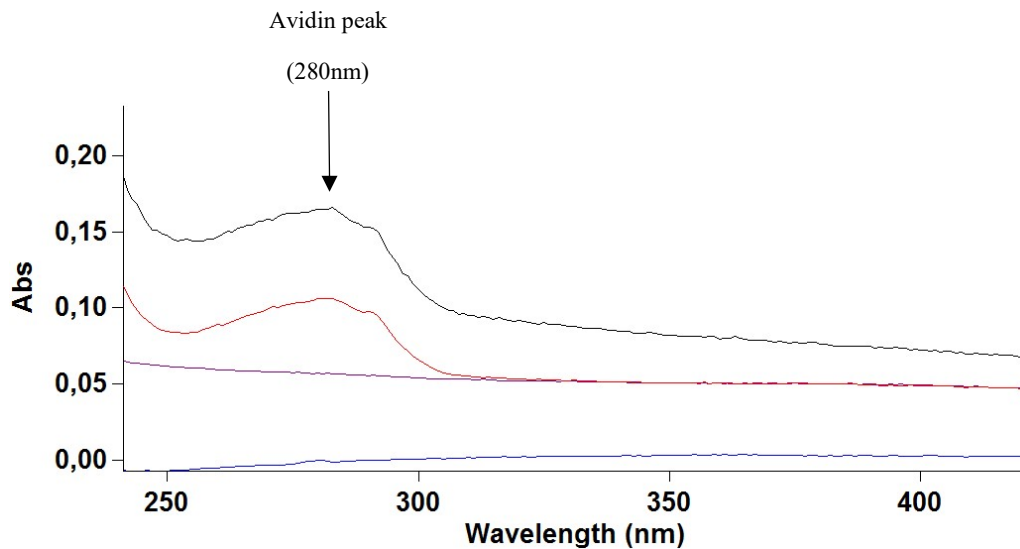


Fig. 4.6. SAMN@avidin spectra. The black spectrum corresponds to the control (only avidin in TMAOH); the red spectrum indicates the supernatant of the SAMN@avidin solution; the blue and violet spectra are the two washes with TMAOH and Milli-Q water.

After the confirmation of the presence of a binding with avidin, SAMN@avidin were derivatized with *Ab-L. monocytogenes*, as described in Paragraph 3.4.2., producing a SAMN@Av@*Ab-L. monocytogenes* complex which was injected at increasing concentrations into the piezoelectric system, without *L. monocytogenes*. The derivatization of SAMN@avidin with the biotinylated antibody against *L. monocytogenes* was performed for the first time. The results were processed by the *Sigma Plot* software. The SAMN@Av@*Ab-L.*

monocytogenes detection in PBS is shown **Fig. 4.7**. The signal decreased, related to the addition of the mass of nanoparticles. This result was useful for understanding the impact of the mass of the nanoparticles in subsequent experiments with bacteria.

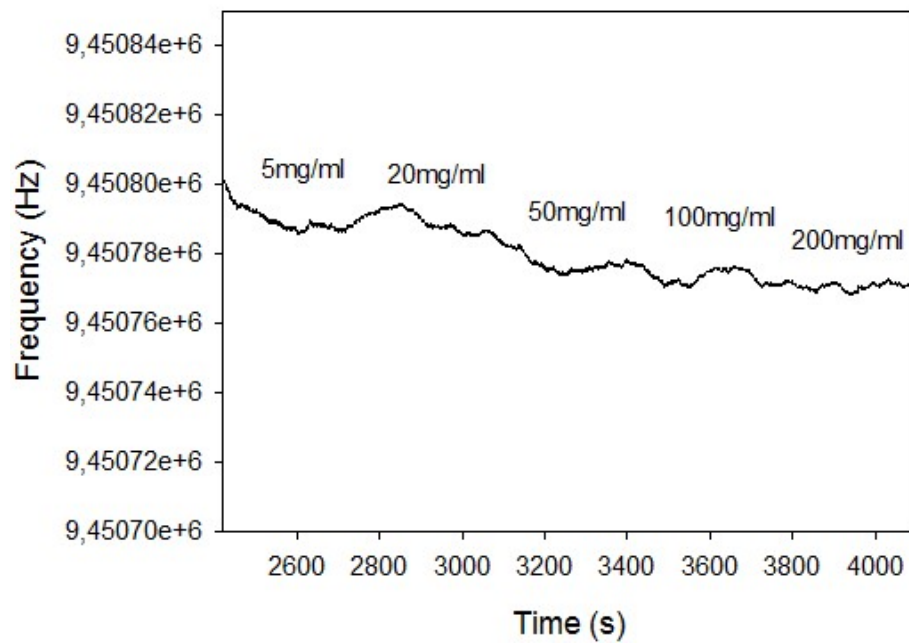


Fig. 4.7. SAMN@Av@Ab-*L. monocytogenes* detection in PBS.

A calibration of the functionalized crystal was performed with SAMN@Av@Ab-*L. monocytogenes* in PBS solution, using different concentrations of SAMN@Av@Ab-*L. monocytogenes*: 1 mg/L, 5 mg/L, 10 mg/L, 30 mg/L, 50 mg/L, 100 mg/L and 200 mg/L. Each concentration was injected in ascending order after the stabilization of the base line, shown by *QC Magic R3*.

After the calibration, two experiments were conducted: the first in PBS and the second in milk.

PBS experiments. In the first experiment, SAMN@Av@Ab-*L. monocytogenes* (100 mg/L) were incubated with different concentrations of *L. monocytogenes*, from $10^{0.5}$ to 10^5 CFU/mL in PBS, for 40 minutes, at room temperature in the dark. The samples were then magnetically isolated for not more than 10 minutes. The pellets were resuspended in PBS. After the stabilization of piezoelectric system, the different samples were injected from $10^{0.5}$ to 10^5 , until crystal saturation. The quartz crystal was previously modified with cysteamine hydrochloride, biotin, avidin and Ab-*L. monocytogenes* for inactivated *L. monocytogenes* detection assays. The results were processed by the *Sigma Plot* software and, as shown in **Fig. 4.8.**, the quartz crystal reached the saturation after the injection of the sample with 10^1 CFU/mL of *L. monocytogenes*. A shift of 120 ΔF was obtained after the introduction of *L. monocytogenes* at $10^{0.5}$ CFU/mL and the injection of *L. monocytogenes* at 10^1 CFU/mL decreased further the frequency of 224 ΔF . In the previous experiment, bacteria were detected on quartz crystal modified with a frequency change of about 2 Hz. It was evident the great amplification effect, due to the increase in mass of nanoparticles.

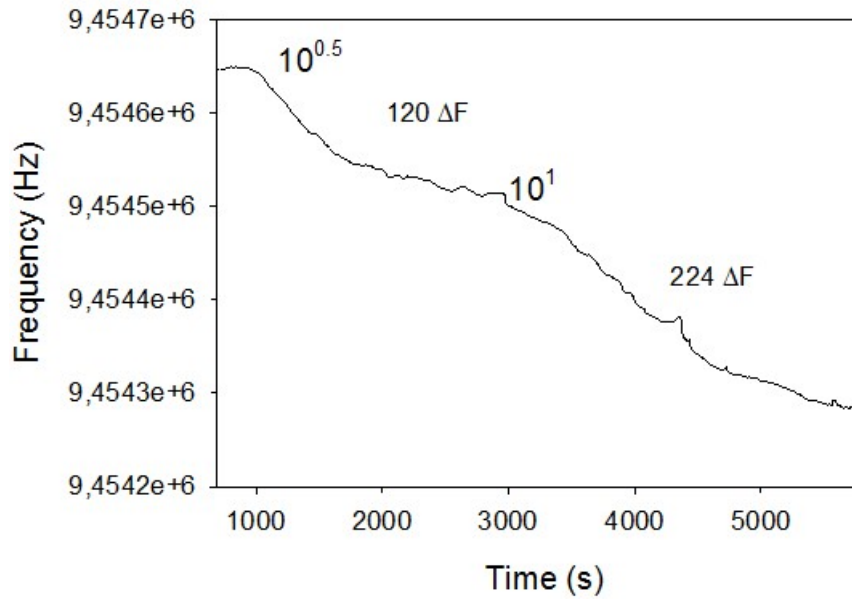


Fig. 4.8. *L. monocytogenes* detection after capture with SAMN@Av@Ab-*L. monocytogenes* in PBS.

The early saturation of crystal didn't permit the acquisition of many points, useful for the construction of the calibration curve. It was not possible to establish a linear correlation between the increasing number of bacterial cells injected and the decreasing values in frequency. Anyway the system revealed a very high sensitivity.

MILK experiments. In the experiment conducted in milk, SAMN@Av@Ab-*L. monocytogenes* (100 mg/L) were incubated with different concentrations of *L. monocytogenes*, from $10^{0.5}$ to 10^5 CFU/mL in milk, for 40 minutes, at room temperature in the dark. The samples were then placed in magnetic separation for not more than 10 minutes. The pellets were resuspended in PBS. After a magnetic separation, pellets were washed two times with PBS to remove

milk residues. Then, they were resuspended in PBS and injected in ascending order of bacterial concentration, until the saturation of the piezoelectric quartz crystal. The quartz crystal was previously modified with cysteamine hydrochloride, biotin, avidin and Ab-*L. monocytogenes* for inactivated *L. monocytogenes* detection assays (see Paragraph 3.3.2). The results have been processed using the *Sigma Plot* software and, as shown in **Fig. 4.9.**, the quartz crystal reached the saturation after the injection of the sample with 10^4 CFU/mL of *L. monocytogenes*,

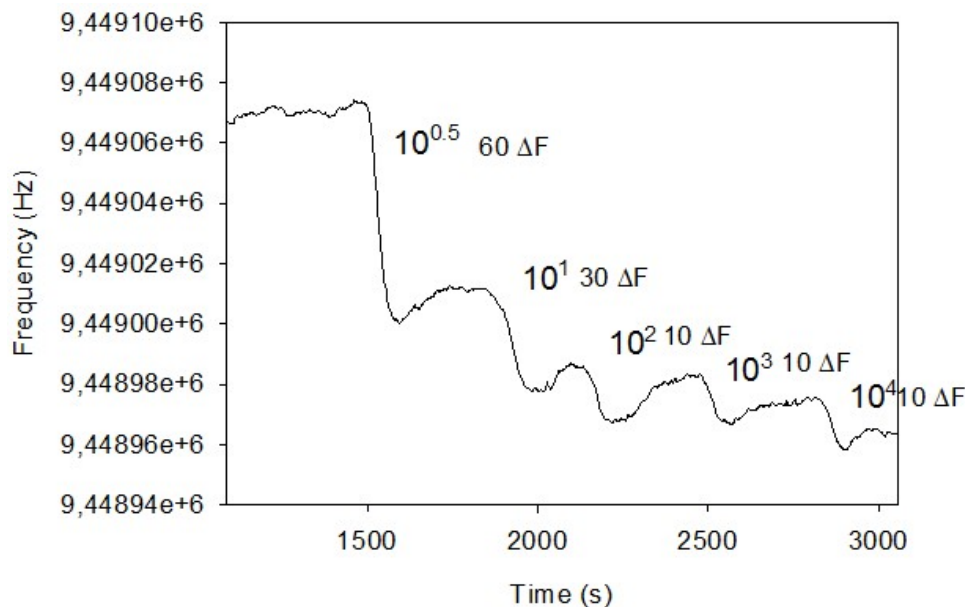


Fig. 4.9. *L. monocytogenes* detection with SAMN@Av@Ab-*L. monocytogenes* in milk.

In the present research, *L. monocytogenes* was detected with a LOD of $10^{0.5}$ CFU/mL (3 cells in 200 μ L of PBS or milk). This result indicates that this

immunosensor can be used to detect *L. monocytogenes* in food rapidly and at a very low concentration, without previous treatments of the substrate. In addition, the use of SAMN@Av@Ab-*L. monocytogenes* has the advantage of amplifying the signal generated on the surface of the piezoelectric quartz crystal.

4.1.3. Reduction of the incubation time of SAMN@Av@Ab-*L. monocytogenes* and *L. monocytogenes*

In the experiments described in the previous Paragraph (4.1.2), the incubation time of SAMN@Av@Ab-*L. monocytogenes* and *L. monocytogenes* was of 40 minutes. The minimum incubation time necessary for the recognition of a low concentration of *L. monocytogenes* (10^1 CFU/mL) in milk by SAMN@Av@Ab-*L. monocytogenes* was tested performing incubations of 3, 6 (**Fig. 4.10.**), 15 and 25 minutes (**Fig. 4.11.**), and the signals displayed by *QC Magic R3* were observed for each incubation.

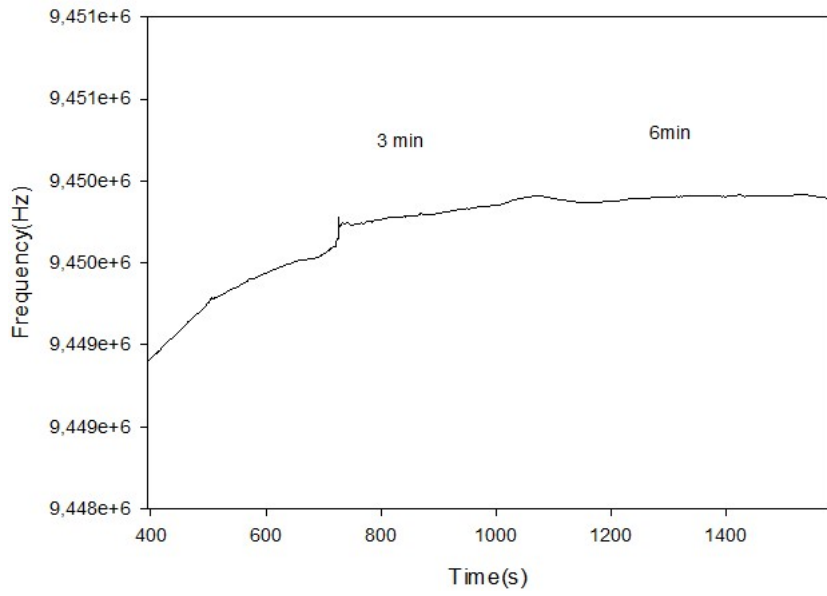


Fig. 4.10. Incubation times of 3 and 6 minutes.

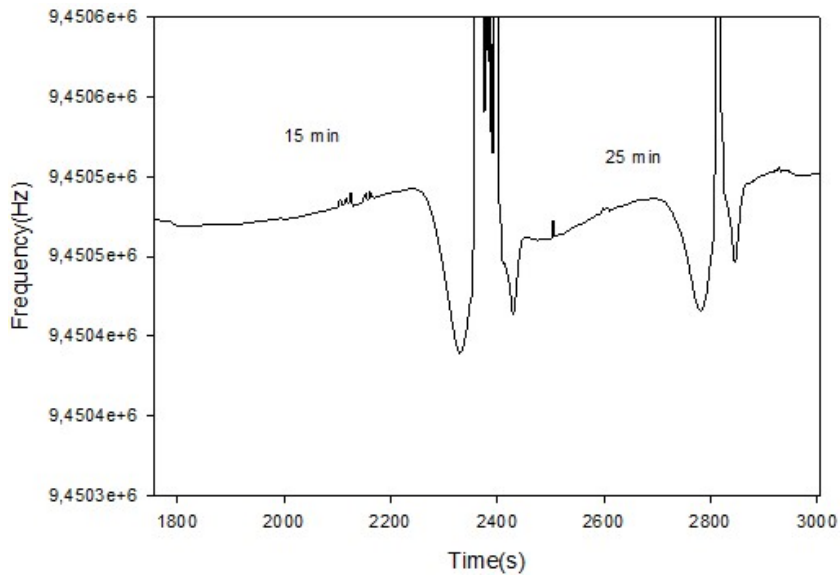


Fig. 4.11. Incubation times of 15 and 25 minutes.

As shown in **Fig. 4.10.**, the incubation times of 3 and 6 minutes were too short for the recognition of *L. monocytogenes* by SAMN@Av@Ab-*L. monocytogenes*. In 15 and 25 minutes, the nanoparticles recognized *L. monocytogenes* but the binding was not stable. Indeed, the signal decreased after the injection of the sample and then it increased. These results indicated that the binding between *L. monocytogenes* and SAMN@Av@Ab-*L. monocytogenes* was not very strong, as a consequence of short incubation times. For this reason, for each experiment conducted in this research, the standard incubation time was of 40 minutes. Nevertheless, it can be considered a very short time compared with the one required by alternative detection techniques, such as culture and plating in selective medium (7 days) and PCR (8-24 hours) [98].

4.1.4. Test of the antibody specificity for *L. monocytogenes*

In order to test and verify the specificity of the biotinylated antibody for the specie *L. monocytogenes*, a procedure similar to the one used in the experiment described in Paragraph 4.1.2. was applied, using the inactivated *L. innocua*. Several concentrations of *L. innocua*, from 10^1 to 10^8 CFU/mL in PBS without SAMNs were injected into the piezoelectric system in ascending order. The results were processed using the *Sigma Plot* software and are shown in **Fig. 4.12**. The signal indicated that biotinylated antibody on the quartz crystal surface did not recognize any concentration of *L. innocua* injected.

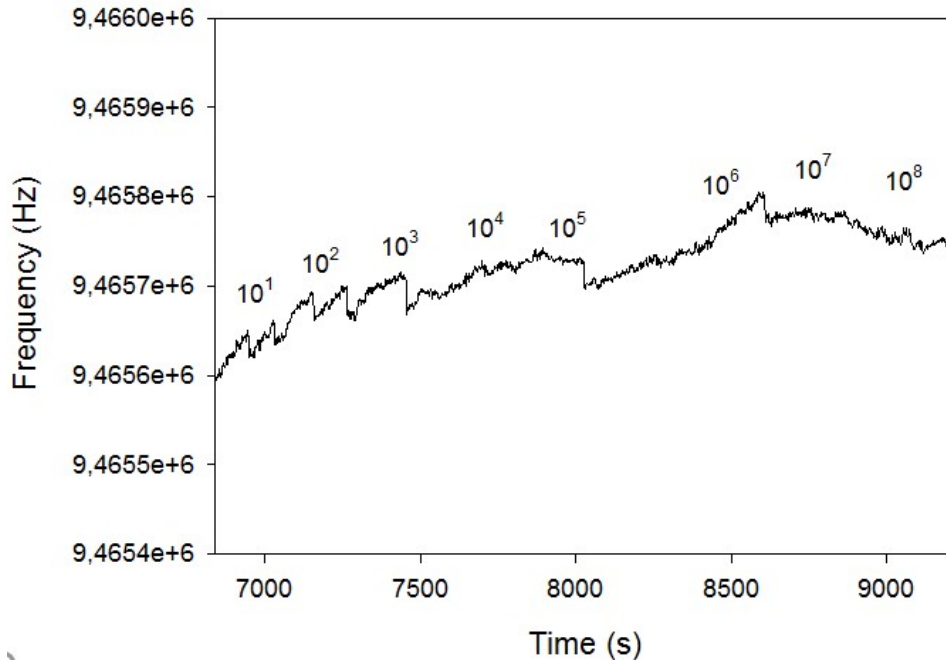


Fig. 4.12. *L. innocua* detection without SAMN@Av@Ab-*L. monocytogenes* in PBS.

Then, SAMN@Av@Ab-*L. monocytogenes* (100 mg/L) were incubated with different concentrations of *L. innocua*, from 10^1 to 10^5 , for 40 minutes, at room temperature in the dark. After a magnetic separation, pellets were resuspended in PBS and injected in ascending order of bacterial concentration. The quartz crystal was modified with cysteamine hydrochloride, biotin, avidin and Ab-*L. monocytogenes* for inactivated *L. innocua* detection assays. Results have been processed using the *Sigma Plot* software (**Fig. 4.13.**).

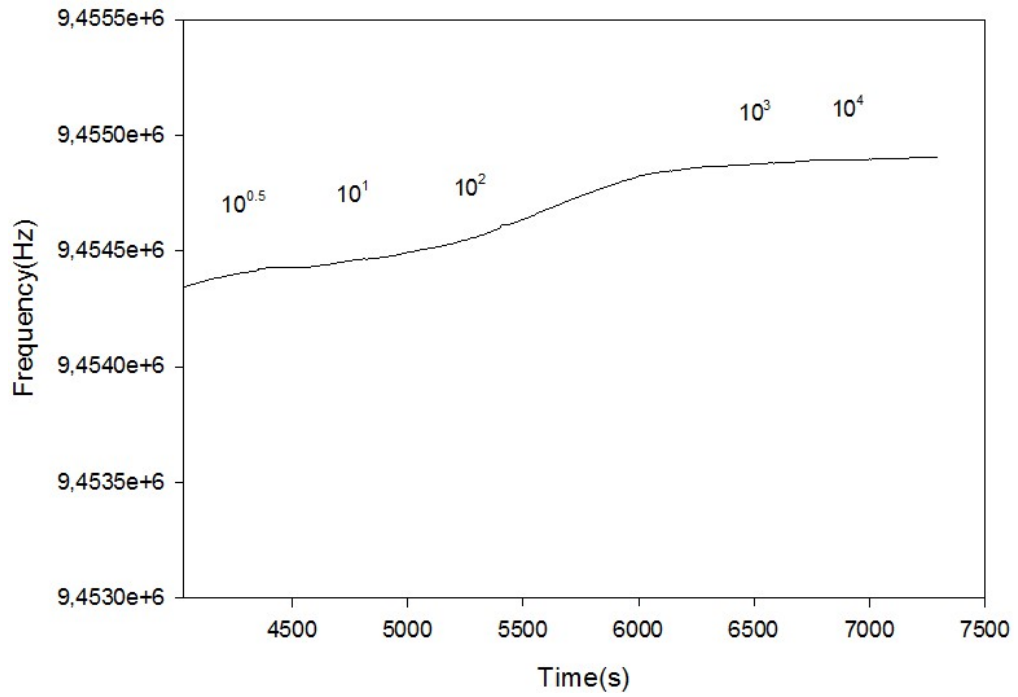


Fig. 4.13. *L. innocua* detection with SAMN@Av@Ab-*L. monocytogenes* in PBS.

No decreases in frequency were recorded, highlighting that the bacteria were not detected by the immunosensor. This led to the conclusion that the biotinylated antibody was specific against *L. monocytogenes*.

4.2. Interaction of SAMNs with live *L. monocytogenes* and Capture efficiency of SAMN@Av@Ab-*L. monocytogenes*

Live bacteria were used to test the ability of SAMNs to capture it in PBS and in milk. Before the capture experiments, it was necessary to verify the absence of toxicity effects on the bacteria, caused by nanoparticles. Previous studies showed that there were no effect of naked nanoparticles on the growth of gram negative bacteria [102]. However, less informations are available on the gram positive, such as *Listeria*. The biotinylated antibody applied in these studies was widely dedicated to the detection of live bacteria. In the present research, only the toxicity experiments were developed only with bare SAMNs.

Different concentrations of bare SAMNs were inoculated with live *L. monocytogenes* with different incubation times, as described in Paragraph 3.5.1. The bacterial concentration of 10^3 CFU/mL, used as starter sample for the experiments, indicated that the sample contained a thousand of cells per mL, an optimal quantity to conduct the three subsequent dilutions. The media used in this experiment were N-AGAR and ALOA. The first is an enrichment medium, in which many species of bacteria can grow. ALOA is a selective medium for *Listeria*. They were used in the experiment to evaluate both the decrease of *L. monocytogenes* concentrations during the incubation times and the possible presence of contaminants into the samples. The experiment was conducted in different incubation times to verify whether SAMNs can caused toxicity to bacterial cells and whether any negative effect can be amplified during the experiment. After

24 hours from the incubation, the bacteria colonies grown were counted, and no contaminants were found.

The results of this experiment led to some important conclusions (**Fig. 4.14**). First, it appeared that SAMNs concentrations tested were no toxic for *L. monocytogenes*. Indeed, the mortality rate of controls (i.e., samples with only *L. monocytogenes*) at time t_6 was comparable to the mortality rate of samples with nanoparticles. Therefore, the progressive mortality detected did not appear to be due to SAMNs. In addition, it was possible to conclude that the most effective concentration of nanoparticles was 100 mg/L.

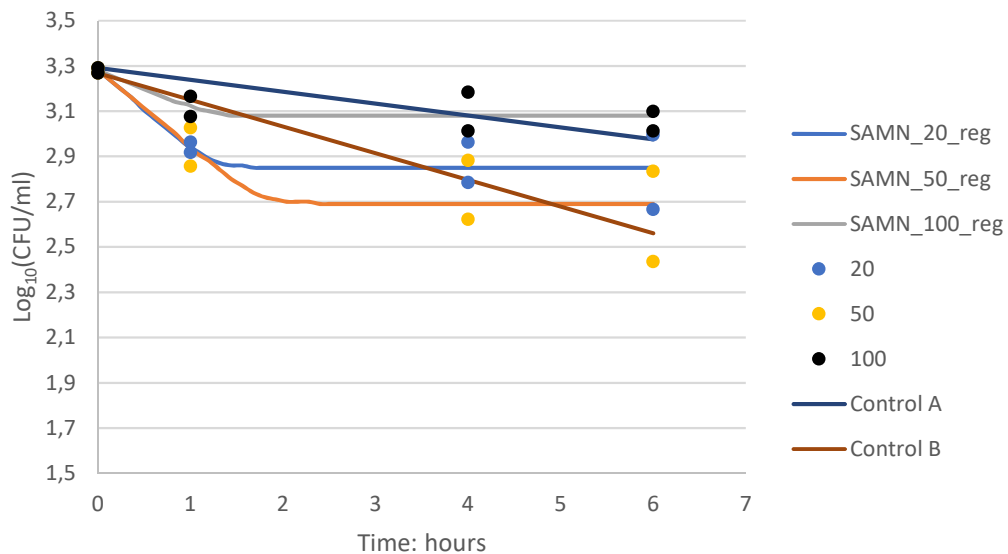


Fig. 4.14. Regression curves of the toxicity experiments.

4.3. Capture of *L. monocytogenes* in PBS: preliminary experiments with SAMNs and SAMN@Av@Ab-*L. monocytogenes*

In order to test the effectiveness of *L. monocytogenes* CE (capture efficiency) with the piezoelectric system, a protocol to capture the live bacteria with bare SAMNs and SAMN@Av@Ab-*L. monocytogenes* in PBS and milk was developed (see Paragraph 3.5.2). After the experiments, the complexes SAMNs - *L. monocytogenes* and SAMN@Av@Ab-*L. monocytogenes* - *L. monocytogenes* were evaluated in terms of supernatants and pellets. The values obtained are listed in **Tab 4.1. and 4.2.**

Tab. 4.1. Recovery efficiency carried out with the bare SAMNs in PBS and milk.

		Supernatant	Pellet	CE%	CE%	NR%	
	LogCFU/mL	Mean±SD	Mean±SD	Supernatant (a)	pellet (b)	Not recovered (c)	
Bacteria concentration CFU/mL							
SAMN 100µg/mL							
	4.6 x10 ⁴	4.66	4.29±0.13	2.74±0.01	55.11	1.33	53.78
	3.5 X 10 ³	3.54	3.22±0.07	2.50±0.16	48.56	9.62	38.95
SAMN 1 g/L							
SAMN PBS							
	9.3 X 10 ³	3.97	3.37±0.13	3.67±0.32	74.56	53.25	21.31
SAMN Milk							
	8.5 X 10 ³	3.93	3.73±0.07	2.34±0.60	23.51	5.48	2.61

(a) Supernatant% = (1-(number of cells from supernatant/total cell number of initial samples)) X 100

(b) Pellet% = (number of cells recovered by pellet/total cell number of initial samples) X 100

(c) Not recovered% = ((total cell number of initial samples-(number of cells recovered by pellet+number of cells from supernatant))/total cell number of initial samples) X 100

Tab. 4.2. Effect of bacterial concentration on the recovery efficiency carried out with the SAMN@Av@Ab-*L. monocytogenes* in PBS.

		Supernatant	Pellet	CE%	CE%	NR%	
	LogCFU/mL	Mean±SD	Mean±SD	Supernatant (a)	pellet (b)	Not recovered (c)	
Bacteria concentration CFU/mL							
	4.6 x10 ⁴	4.66	4.33±0.26	3.07±0.38	51.38	2.80	48.59
	3.5 X 10 ³	3.54	3.40±0.27	1.84±0.41	23.04	2.25	20.80
	1.1 X 10 ²	2.07	1.89±0.03	0.84±0.0	33.36	5.91	27.45

(a) Supernatant% = (1-(number of cells from supernatant/total cell number of initial samples)) X 100

(b) Pellet % = (number of cells recovered by pellet/total cell number of initial samples) X 100

(c) Not recovered% = ((total cell number of initial samples-(number of cells recovered by pellet+number of cells from supernatant))/total cell number of initial samples) X 100

Data are referred on TSAYE medium.

These values showed that bonds between nanoparticles and *L. monocytogenes* were formed with a bacterial concentration of 10^3 and 10^4 CFU/mL. Bonds were quantified by CE% values from 74 to 55% of recovered cells. This depended also by the SAMNs concentrations (100 μ g vs 1 g). The CE% values differed among the media applied for the cell recovery. ALOA showed the worst values of recovery bacteria also in the control samples. This is due to the sub-lethal stress induced by the selective compounds of the ALOA [103].

For this reasons, the data are reported only for the TSAYE medium in the **Tab. 4.1**. The bare SAMNs showed a great affinity for bacteria live cells however this is not a specific linkage. Moreover, the CE values were dramatically reduced when the naked SAMNs were applied to the milk matrix.

The CE values of the SAMN@Av@Ab-*L. monocytogenes* in the PBS medium were showed in **Tab. 4.2**. The specific linkage with antibody and live bacteria showed that the CE values ranged from the 33 to the 55%.

The bacterial concentration selected for the subsequent studies is 10^3 UFC/mL, this level of bacterial concentration can be easily managed by the plate count methods without problems related to the limit of detection of the cultural methods.

At the end of the experiment, eppendorfs containing pellets were washed with PBS and then incubated with their three subsequent dilutions both in ALOA and TSBYE at 37°C for 24 hours, in order to test whether bacterial cells remained linked to the plastic tube or not. No bacterial colonies were detected in plates: this was a clear indicator that bacteria did not adhere to eppendorfs.

4.4. Capture test with different concentrations of SAMN@Av@Ab-*L. monocytogenes* on milk samples

SAMNs derivatized with biotinylated antibody were used to evaluate the feasibility of the magnetic separation of the live bacterial cells from PBS and milk. This pre-treatment of nanoparticles permitted to concentrate *L. monocytogenes* and to amplify the signal of the piezoelectric quartz crystal. In addition, the magnetic separation conducted with SAMNs was avoided to capture *L. monocytogenes* in very low concentration. Two different concentrations of SAMN@Av@Ab-*L. monocytogenes* were incubated with bacteria, as described in Paragraph 3.5.3., to evaluate the existence of possible differences between them. This experiment was performed first in PBS and then in milk, and the number of recovered cells was estimate. As previously reported, the data collected from the non-selective medium (TSBYE) was used, because the real amount of recovered *L. monocytogenes* cells retained by nanoparticles could be underestimated in the selective medium (ALOA).

Moreover, other factors can affect the CE% such as the possible formation of cell clusters and other aggregation effects on the surface of SAMNs during the magnetic separation [104]. The percentage of recovered cells in the experiment performed in PBS with a nanoparticles concentration of 100 mg/L is showed in **Tab. 4.1**. The same percentage is showed for the experiment conducted in milk. The supernatant percentage is unaffected by the formation of cells clusters or by any other lethal effect, due to the cells deformation. This index was useful to

calculate the percentage of capture efficiency (CE) [97]. The values of CE and NR were reported in **Tab. 4.1**.

CONCLUSIONS

In the present research work, a piezoelectric quartz crystal modified with Ab-*L. monocytogenes* permitted to detect known concentrations of inactivated *L. monocytogenes* in milk. Assays were performed in real time, without samples' pre-treatments, showing high sensitivity. The proposed system presented several advantages, as the low cost of materials, the ease of use without specific devices and the possibility to use each surface of the crystal for two different assays. Several derivatizations were performed on quartz crystal, but the functionalization with the biotinylated antibody was the most effective for *L. monocytogenes* detection. Indeed, bare quartz crystal didn't detect any concentration of bacteria injected, while the modified crystal shown a clear decrease in frequency for each concentration injected of *L. monocytogenes*.

Novel complexes, such as SAMN@avidin and SAMN@Av@Ab-*L. monocytogenes*, were produced and characterized identifying the optimal conditions for their formation and function. Complexes were quantified and characterized by analytical techniques, such as spectrophotometer and piezoelectric system. The spectrophotometer permitted to observe whether the binding has taken place, while the piezoelectric system allowed to understand the efficiency of this binding. SAMN@Av@Ab-*L. monocytogenes* were used to capture inactivated *L. monocytogenes* first in PBS and then in milk. Magnetic nanoparticles coupled with the piezoelectric system, amplified significantly the signal and allowed to detect

low concentration of bacteria in samples (less of 10 cells/mL). This method can be coupled with a microbiological one, such as the traditional plate count performed in two media, one selective (ALOA) and one non-selective (TSBYE). However, the modified crystal reached the saturation earlier, so that it was not possible to build a calibration curve for the lack of acquisition points during the measurement. This suggested the need to improve the crystal washing system removing samples residues, which may interfere with the signal. Further evidences of the experiment strength into the food matrix are thus necessary. In addition, the biotinylated antibody specific for *L. monocytogenes*, currently is not commercially available, as the specific antigen recognized by the biotinylated antibody used for this experiment is unknown.

The reported results were encouraging, but the preliminary nature of the present study highlights the need of further implementations. For example, different concentrations of SAMN@Av@Ab-*L. monocytogenes* incubated with different concentrations of *L. monocytogenes* should be tested. Finally, the possibility to coat the magnetic nanoparticles with others specific compounds or performing some pre-treatments on the samples should be explored.

BIBLIOGRAPHY

- [1] Myers, R. J. (2009). One-hundred years of pH. *Journal of Chemical Education*, 87(1), 30-32.
- [2] Buerk, D. G. (1995). *Biosensors: Theory and applications*. Crc Press.
- [3] Heyrovský, J., & Kuřta, J. (2013). *Principles of polarography*. Elsevier.
- [4] Clark Jr, L. C. (2004). *U.S. Patent No. 6,815,186*. Washington, DC: U.S. Patent and Trademark Office.
- [5] Taitt, C. R., Anderson, G. P., & Ligler, F. S. (2016). Evanescent wave fluorescence biosensors: Advances of the last decade. *Biosensors and Bioelectronics*, 76, 103-112.
- [6] Cornell, B. A., Braach-Maksvytis, V. L. B., King, L. G., Osman, P. D. J., Raguse, B., Wieczorek, L., & Pace, R. J. (1997). A biosensor that uses ion-channel switches. *NATURE-LONDON-*, 580-582.
- [7] Kubik, T., Bogunia-Kubik, K., & Sugisaka, M. (2005). Nanotechnology on duty in medical applications. *Current pharmaceutical biotechnology*, 6(1), 17-33.
- [8] Book, G., 2014, Compendium of Chemical Terminology. *International Union of Pure and Applied Chemistry*.
- [9] Mann, S. (1993). Molecular tectonics in biomineralization and biomimetic materials chemistry. *Nature*, 365(6446), 499-505.
- [10] Love, J. C., Estroff, L. A., Kriebel, J. K., Nuzzo, R. G., & Whitesides, G. M. (2005). Self-assembled monolayers of thiolates on metals as a form of nanotechnology. *Chemical reviews*, 105(4), 1103-1170.

- [11] Blodgett, K. B. (1934). Monomolecular films of fatty acids on glass. *Journal of the American Chemical Society*, 56(2), 495-495.
- [12] Bigelow, W. C., Pickett, D. L., & Zisman, W. A. (1946). Oleophobic monolayers: I. Films adsorbed from solution in non-polar liquids. *Journal of Colloid Science*, 1(6), 513-538.
- [13] Allara, D. L., & Nuzzo, R. G. (1985). Spontaneously organized molecular assemblies. 1. Formation, dynamics, and physical properties of n-alkanoic acids adsorbed from solution on an oxidized aluminum surface. *Langmuir*, 1(1), 45-52.
- [14] Wasserman, S. R., Tao, Y. T., & Whitesides, G. M. (1989). Structure and reactivity of alkylsiloxane monolayers formed by reaction of alkyltrichlorosilanes on silicon substrates. *Langmuir*, 5(4), 1074-1087.
- [15] Lee, H., Kepley, L. J., Hong, H. G., Akhter, S., & Mallouk, T. E. (1988). Adsorption of ordered zirconium phosphonate multilayer films on silicon and gold surfaces. *The Journal of Physical Chemistry*, 92(9), 2597-2601.
- [16] Nuzzo, R. G., & Allara, D. L. (1983). Adsorption of bifunctional organic disulfides on gold surfaces. *Journal of the American Chemical Society*, 105(13), 4481-4483.
- [17] Fendler, J. H. (1996). Self-assembled nanostructured materials. *Chemistry of Materials*, 8(8), 1616-1624.
- [18] Colvin, V. L., Goldstein, A. N., & Alivisatos, A. P. (1992). Semiconductor nanocrystals covalently bound to metal surfaces with self-assembled monolayers. *Journal of the American Chemical Society*, 114(13), 5221-5230.
- [19] Ulman, A. (1996). Formation and structure of self-assembled monolayers. *Chemical reviews*, 96(4), 1533-1554.

- [20] Ferretti, S., Paynter, S., Russell, D. A., Sapsford, K. E., & Richardson, D. J. (2000). Self-assembled monolayers: a versatile tool for the formulation of bio-surfaces. *TrAC Trends in Analytical Chemistry*, 19(9), 530-540.
- [21] Hodneland, C. D., Lee, Y. S., Min, D. H., & Mrksich, M. (2002). Selective immobilization of proteins to self-assembled monolayers presenting active site-directed capture ligands. *Proceedings of the National Academy of Sciences*, 99(8), 5048-5052.
- [22] White, H. 3., & Whitehead, C. C. (1987). Role of avidin and other biotin-binding proteins in the deposition and distribution of biotin in chicken eggs. Discovery of a new biotin-binding protein. *Biochemical Journal*, 241(3), 677-684.
- [23] Zemleni, J., & Mock, D. (1999). Biotin biochemistry and human requirements. *The Journal of nutritional biochemistry*, 10(3), 128-138.
- [24] Livaniou, E., Costopoulou, D., Vassiliadou, I., Leondiadis, L., Nyalala, J. O., Ithakissios, D. S., & Evangelatos, G. P. (2000). Analytical techniques for determining biotin. *Journal of Chromatography A*, 881(1), 331-343.
- [25] Pacheco-Alvarez, D., Solórzano-Vargas, R. S., & Del Río, A. L. (2002). Biotin in metabolism and its relationship to human disease. *Archives of medical research*, 33(5), 439-447.
- [26] Dakshinamurti, K. (2005). Biotin—a regulator of gene expression. *The Journal of nutritional biochemistry*, 16(7), 419-423.
- [27] León-Del-Río, A. (2005). Biotin-dependent regulation of gene expression in human cells. *The Journal of nutritional biochemistry*, 16(7), 432-434.
- [28] Ho, R. C., & Cordain, L. (2000). The potential role of biotin insufficiency on essential fatty acid metabolism and cardiovascular disease risk. *Nutrition Research*, 20(8), 1201-1212.

- [29] Schutte, A. E., van Rooyen, J. M., Huisman, H. W., Kruger, H. S., & Malan, N. T. (2007). The potential role of biotin as dietary risk marker for hypertension in black South African children—the THUSA BANA study. *South African Journal of Clinical Nutrition*.
- [30] Gravel, R. A., & Narang, M. A. (2005). Molecular genetics of biotin metabolism: old vitamin, new science. *The Journal of nutritional biochemistry*, 16(7), 428-431.
- [31] Zerega, B., Camardella, L., Cermelli, S., Sala, R., Cancedda, R., & Cancedda, F. D. (2001). Avidin expression during chick chondrocyte and myoblast development in vitro and in vivo: regulation of cell proliferation. *Journal of cell science*, 114(8), 1473-1482.
- [32] Gope, M. L., Keinänen, R. A., Kristn, P. A., Conneely, O. M., Beattie, W. G., Zarucki-Schulz, T., ... & Kulomaa, M. S. (1987). Molecular cloning of the chicken avidin cDNA. *Nucleic acids research*, 15(8), 3595-3606.
- [33] Elo, H. A., Räisänen, S., & Tuohimaa, P. J. (1980). Induction of an antimicrobial biotin-binding egg white protein (avidin) in chick tissues in septic *Escherichia coli* infection. *Experientia*, 36(3), 312-313.
- [34] Elo, H., & Tuohimaa, P. (1974). An improved micro-method for avidin assay. *Biochemical Journal*, 140(1), 115-116.
- [35] Green, N. M. (1975). Avidin. *Advances in protein chemistry*, 29, 85-133.
- [36] Goldman, E. R., Balighian, E. D., Mattoussi, H., Kuno, M. K., Mauro, J. M., Tran, P. T., & Anderson, G. P. (2002). Avidin: a natural bridge for quantum dot-antibody conjugates. *Journal of the American Chemical Society*, 124(22), 6378-6382.

- [37] Korpela, J., Kulomaa, M., Tuohimaa, P., & Vaheri, A. (1983). Avidin is induced in chicken embryo fibroblasts by viral transformation and cell damage. *The EMBO journal*, 2(10), 1715.
- [38] Livnah, O., Bayer, E. A., Wilchek, M., & Sussman, J. L. (1993). Three-dimensional structures of avidin and the avidin-biotin complex. *Proceedings of the National Academy of Sciences*, 90(11), 5076-5080.
- [39] Hsu, S. M., Raine, L., & Fanger, H. (1981). Use of avidin-biotin-peroxidase complex (ABC) in immunoperoxidase techniques: a comparison between ABC and unlabeled antibody (PAP) procedures. *Journal of Histochemistry & Cytochemistry*, 29(4), 577-580.
- [40] Dontha, N., Nowall, W. B., & Kuhr, W. G. (1997). Generation of biotin/avidin/enzyme nanostructures with maskless photolithography. *Analytical chemistry*, 69(14), 2619-2625.
- [41] Kergaravat, S. V., Gómez, G. A., Fabiano, S. N., Chávez, T. I. L., Pividori, M. I., & Hernández, S. R. (2012). Biotin determination in food supplements by an electrochemical magneto biosensor. *Talanta*, 97, 484-490.
- [42] Chamberlain, K. (2004). Food and health: Expanding the agenda for health psychology. *Journal of Health Psychology*, 9(4), 467-481.
- [43] Yeung, R. M., & Morris, J. (2001). Food safety risk: Consumer perception and purchase behaviour. *British Food Journal*, 103(3), 170-187.
- [44] Grunert, K. G. (2005). Food quality and safety: consumer perception and demand. *European Review of Agricultural Economics*, 32(3), 369-391.
- [45] Mead, P. S., Slutsker, L., Dietz, V., McCaig, L. F., Bresee, J. S., Shapiro, C., ... & Tauxe, R. V. (1999). Food-related illness and death in the United States. *Emerging infectious diseases*, 5(5), 607.

- [46] Antle, J. M. (1999). Benefits and costs of food safety regulation. *Food policy*, 24(6), 605-623.
- [47] Centers for Disease Control and Prevention (CDC) (2010). Preliminary FoodNet data on the incidence of infection with pathogens transmitted commonly through food-10 states, 2009. *MMWR. Morbidity and mortality weekly report*, 59(14), 418.
- [48] Farber, J. M., & Peterkin, P. I. (1991). *Listeria monocytogenes*, a food-borne pathogen. *Microbiological reviews*, 55(3), 476-511.
- [49] Gray, M. L., & Killinger, A. H. (1966). *Listeria monocytogenes* and listeric infections. *Bacteriological reviews*, 30(2), 309.
- [50] Ryser, E. T., & Marth, E. H. (Eds.). (2007). *Listeria, listeriosis, and food safety*. CRC Press.
- [51] Gibbons, N. E. (1972). *Listeria Pirie* - Whom Does It Honor?. *International Journal of Systematic and Evolutionary Microbiology*, 22(1), 1-3.
- [52] Todar, K. (2015). Textbook of bacteriology.
- [53] McLauchlin, J., Rees, C. E., & Dodd, C. E. (2014). *Listeria monocytogenes* and the genus *Listeria*. In *The Prokaryotes* (pp. 241-259). Springer Berlin Heidelberg.
- [54] Olier, M., Pierre, F., Rousseaux, S., Lemaître, J. P., Rousset, A., Piveteau, P., & Guzzo, J. (2003). Expression of truncated internalin A is involved in impaired internalization of some *Listeria monocytogenes* isolates carried asymptotically by humans. *Infection and immunity*, 71(3), 1217-1224.
- [55] Buchrieser, C. (2007). Biodiversity of the species *Listeria monocytogenes* and the genus *Listeria*. *Microbes and Infection*, 9(10), 1147-1155.

- [56] Glaser, P., Frangeul, L., Buchrieser, C., Rusniok, C., Amend, A., Baquero, F., ... & Charbit, A. (2001). Comparative genomics of *Listeria* species. *Science*, 294(5543), 849-852.
- [57] Nelson, K. E., Fouts, D. E., Mongodin, E. F., Ravel, J., DeBoy, R. T., Kolonay, J. F., ... & Peterson, J. (2004). Whole genome comparisons of serotype 4b and 1/2a strains of the food-borne pathogen *Listeria monocytogenes* reveal new insights into the core genome components of this species. *Nucleic acids research*, 32(8), 2386-2395.
- [58] Cabanes, D., Dehoux, P., Dussurget, O., Frangeul, L., & Cossart, P. (2002). Surface proteins and the pathogenic potential of *Listeria monocytogenes*. *Trends in microbiology*, 10(5), 238-245.
- [59] Leimeister-Wächter, M., Domann, E., & Chakraborty, T. (1992). The expression of virulence genes in *Listeria monocytogenes* is thermoregulated. *Journal of bacteriology*, 174(3), 947-952.
- [60] Johansson, J., Mandin, P., Renzoni, A., Chiaruttini, C., Springer, M., & Cossart, P. (2002). An RNA thermosensor controls expression of virulence genes in *Listeria monocytogenes*. *Cell*, 110(5), 551-561.
- [61] Cossart, P., & Toledo-Arana, A. (2008). *Listeria monocytogenes*, a unique model in infection biology: an overview. *Microbes and Infection*, 10(9), 1041-1050.
- [62] Southwick, F. S., & Purich, D. L. (1996). Intracellular pathogenesis of listeriosis. *New England Journal of Medicine*, 334(12), 770-776.
- [63] Rocourt, J., Jacquet, C., & Reilly, A. (2000). Epidemiology of human listeriosis and seafoods. *International journal of food microbiology*, 62(3), 197-209.

- [64] Conlan, J. W., & North, R. J. (1991). Neutrophil-mediated dissolution of infected host cells as a defense strategy against a facultative intracellular bacterium. *Journal of Experimental Medicine*, 174(3), 741-744.
- [65] Cossart, P., & Lecuit, M. (1998). Interactions of *Listeria monocytogenes* with mammalian cells during entry and actin-based movement: bacterial factors, cellular ligands and signaling. *The EMBO journal*, 17(14), 3797-3806.
- [66] Regulation, E. U. (2005). 2073/2005 of 15 November 2005 on microbiological criteria for foodstuffs. *Official Journal of the European Union*, 338, 1-29.
- [67] Beumer, R. R., & Hazeleger, W. C. (2003). *Listeria monocytogenes*: diagnostic problems. *FEMS Immunology & Medical Microbiology*, 35(3), 191-197.
- [68] Meyer, R. R., Probst, G. S., & Keller, S. J. (1972). RNA synthesis by isolated mammalian mitochondria and nuclei: effects of ethidium bromide and acriflavin. *Archives of biochemistry and biophysics*, 148(2), 425-430.
- [69] Fraser, J. A., & Sperber, W. H. (1988). Rapid detection of *Listeria* spp. in food and environmental samples by esculin hydrolysis. *Journal of Food Protection*®, 51(10), 762-765.
- [70] Scotter, S. L., Langton, S., Lombard, B., Lahellec, C., Schulten, S., Nagelkerke, N., ... & Rollier, P. (2001). Validation of ISO method 11290: Part 2. Enumeration of *Listeria monocytogenes* in foods. *International journal of food microbiology*, 70(1), 121-129.
- [71] Rossmannith, P., Krassnig, M., Wagner, M., & Hein, I. (2006). Detection of *Listeria monocytogenes* in food using a combined enrichment/real-time PCR method targeting the *prfA* gene. *Research in Microbiology*, 157(8), 763-771.

- [72] Rodríguez-Lázaro, D., Jofré, A., Aymerich, T., Hugas, M., & Pla, M. (2004). Rapid quantitative detection of *Listeria monocytogenes* in meat products by real-time PCR. *Applied and Environmental Microbiology*, 70(10), 6299-6301.
- [73] Välimaa, A. L., Tilsala-Timisjärvi, A., & Virtanen, E. (2015). Rapid detection and identification methods for *Listeria monocytogenes* in the food chain—A review. *Food Control*, 55, 103-114.
- [74] Sue, M. J., Yeap, S. K., Omar, A. R., & Tan, S. W. (2014). Application of PCR-ELISA in molecular diagnosis. *BioMed research international*, 2014.
- [75] Scheu, P., Gasch, A., & Berghof, K. (1999). Rapid detection of *Listeria monocytogenes* by PCR-ELISA. *Letters in applied microbiology*, 29(6), 416-420.
- [76] Kim, S. H., Park, M. K., Kim, J. Y., Chuong, P. D., Lee, Y. S., Yoon, B. S., ... & Lim, Y. K. (2005). Development of a sandwich ELISA for the detection of *Listeria* spp. using specific flagella antibodies. *J. Vet. Sci*, 6(1), 41-46.
- [77] O'sullivan, C. K., & Guilbault, G. G. (1999). Commercial quartz crystal microbalances—theory and applications. *Biosensors and bioelectronics*, 14(8), 663-670.
- [78] Tsai, H., Lin, Y., Chang, H. W., & Fuh, C. B. (2008). Integrating the QCM detection with magnetic separation for on-line analysis. *Biosensors and Bioelectronics*, 24(3), 485-488.
- [79] Konash, P. L., & Bastiaans, G. J. (1980). Piezoelectric crystals as detectors in liquid chromatography. *Analytical chemistry*, 52(12), 1929-1931.
- [80] Voinova, M. V., Jonson, M., & Kasemo, B. (2002). 'Missing mass' effect in biosensor's QCM applications. *Biosensors and Bioelectronics*, 17(10), 835-841.
- [81] Kankare, J. (2002). Sauerbrey equation of quartz crystal microbalance in liquid medium. *Langmuir*, 18(18), 7092-7094.

- [82] Saad, N. A., Zaaba, S. K., Zakaria, A., Kamarudin, L. M., Wan, K., & Shariman, A. B. (2014, August). Quartz crystal microbalance for bacteria application review. In *Electronic Design (ICED), 2014 2nd International Conference on* (pp. 455-460). IEEE.
- [83] Shen, G., Liu, M., Cai, X., & Lu, J. (2008). A novel piezoelectric quartz crystal immuno sensor based on hyperbranched polymer films for the detection of α -Fetoprotein. *Analytica chimica acta*, 630(1), 75-81.
- [84] Hasanzadeh, M., Shadjou, N., & de la Guardia, M. (2015). Iron and iron-oxide magnetic nanoparticles as signal-amplification elements in electrochemical biosensing. *TrAC Trends in Analytical Chemistry*, 72, 1-9.
- [85] Wittenberg, N. J., & Haynes, C. L. (2009). Using nanoparticles to push the limits of detection. *Wiley Interdisciplinary Reviews: Nanomedicine and Nanobiotechnology*, 1(2), 237-254.
- [86] Shao, H., Min, C., Issadore, D. A., Liong, M., Yoon, T. J., Weissleder, R., & Lee, H. (2012). Magnetic nanoparticles and microNMR for diagnostic applications.
- [87] Osaka, T., Matsunaga, T., Nakanishi, T., Arakaki, A., Niwa, D., & Iida, H. (2006). Synthesis of magnetic nanoparticles and their application to bioassays. *Analytical and bioanalytical chemistry*, 384(3), 593-600.
- [88] Gupta, A. K., & Gupta, M. (2005). Synthesis and surface engineering of iron oxide nanoparticles for biomedical applications. *Biomaterials*, 26(18), 3995-4021.
- [89] Cao, M., Li, Z., Wang, J., Ge, W., Yue, T., Li, R., ... & William, W. Y. (2012). Food related applications of magnetic iron oxide nanoparticles: enzyme immobilization, protein purification, and food analysis. *Trends in Food Science & Technology*, 27(1), 47-56.

- [90] Emrani, A. S., Danesh, N. M., Lavaee, P., Ramezani, M., Abnous, K., & Taghdisi, S. M. (2016). Colorimetric and fluorescence quenching aptasensors for detection of streptomycin in blood serum and milk based on double-stranded DNA and gold nanoparticles. *Food chemistry*, *190*, 115-121.
- [91] Freitas, M., Viswanathan, S., Nouws, H. P. A., Oliveira, M. B. P. P., & Delerue-Matos, C. (2014). Iron oxide/gold core/shell nanomagnetic probes and CdS biolabels for amplified electrochemical immunosensing of *Salmonella typhimurium*. *Biosensors and Bioelectronics*, *51*, 195-200.
- [92] Magro, M., Faralli, A., Baratella, D., Bertipaglia, I., Giannetti, S., Salviulo, G., ... & Vianello, F. (2012). Avidin functionalized maghemite nanoparticles and their application for recombinant human biotinyl-SERCA purification. *Langmuir*, *28*(43), 15392-15401.
- [93] Magro, M., Sinigaglia, G., Nodari, L., Tucek, J., Polakova, K., Marusak, Z., ... & Zboril, R. (2012). Charge binding of rhodamine derivative to OH⁻ stabilized nanomaghemite: universal nanocarrier for construction of magnetofluorescent biosensors. *Acta biomaterialia*, *8*(6), 2068-2076.
- [94] Schladt, T. D., Schneider, K., Schild, H., & Tremel, W. (2011). Synthesis and bio-functionalization of magnetic nanoparticles for medical diagnosis and treatment. *Dalton Transactions*, *40*(24), 6315-6343.
- [95] Datta, S. K., Okamoto, S., Hayashi, T., Shin, S. S., Mihajlov, I., Fermin, A., ... & Raz, E. (2006). Vaccination with irradiated *Listeria* induces protective T cell immunity. *Immunity*, *25*(1), 143-152.
- [96] Baranyi J. and Roberts T.A. 1994. A dynamic approach to predicting bacterial growth in food. *Int. J. Food Microbiol.* *23*, 277-294.

- [97] Shan, S., Zhong, Z., Lai, W., Xiong, Y., Cui, X., & Liu, D. (2014). Immunomagnetic nanobeads based on a streptavidin-biotin system for the highly efficient and specific separation of *Listeria monocytogenes*. *Food Control*, *45*, 138-142.
- [98] Yang, H., Qu, L., Wimbrow, A. N., Jiang, X., & Sun, Y. (2007). Rapid detection of *Listeria monocytogenes* by nanoparticle-based immunomagnetic separation and real-time PCR. *International Journal of Food Microbiology*, *118*(2), 132-138.
- [99] Hao, R., Wang, D., Zhang, X. E., Zuo, G., Wei, H., Yang, R., ... & Zhou, Y. (2009). Rapid detection of *Bacillus anthracis* using monoclonal antibody functionalized QCM sensor. *Biosensors and Bioelectronics*, *24*(5), 1330-1335.
- [100] Buchatip, S., Ananthanawat, C., Sithigorngul, P., Sangvanich, P., Rengpipat, S., & Hoven, V. P. (2010). Detection of the shrimp pathogenic bacteria, *Vibrio harveyi*, by a quartz crystal microbalance-specific antibody based sensor. *Sensors and Actuators B: Chemical*, *145*(1), 259-264.
- [101] Sharma, H., & Mutharasan, R. (2013). Rapid and sensitive immunodetection of *Listeria monocytogenes* in milk using a novel piezoelectric cantilever sensor. *Biosensors and Bioelectronics*, *45*, 158-162.
- [102] Magro, M., Fasolato, L., Bonaiuto, E., Andreani, N. A., Baratella, D., Corraducci, V., ... & Vianello, F. (2016). Enlightening mineral iron sensing in *Pseudomonas fluorescens* by surface active maghemite nanoparticles: Involvement of the OprF porin. *Biochimica et Biophysica Acta (BBA)-General Subjects*, *1860*(10), 2202-2210.
- [103] Jasson, V., Uyttendaele, M., Rajkovic, A., & Debevere, J. (2007). Establishment of procedures provoking sub-lethal injury of *Listeria*

monocytogenes, *Campylobacter jejuni* and *Escherichia coli* O157 to serve method performance testing. *International Journal of Food Microbiology*, 118(3), 241-249.

[104] Varshney, M., Yang, L., Su, X. L., & Li, Y. (2005). Magnetic nanoparticle-antibody conjugates for the separation of *Escherichia coli* O157: H7 in ground beef. *Journal of food protection*, 68(9), 1804-1811.

ACKNOWLEDGEMENTS

After five years, I can say that I am happy. I reached an important goal, supported by who made me better. Thanks dad, for the precious time that life has granted us to spend together and for conveying to me the curiosity and the force to continue along the way of my life. Thanks mum, for encouraging me to follow my dreams, for your comprehension and sweetness. Thanks Ale, for your constant presence and to be the sister who everyone should have. Thanks Enrico, for giving me so many smiles. Thanks Daniela, to animate my culinary fantasies.

Days at the university and nights on Whatsapp would not be the same without you, Ele, Bene, Auri, Sofi and Elisa. I won against *Listeria* thanks to you Mary and Marco. Lauri, I'm honoured to be your Friend.

Va, Bibi, Pix and Ele thanks to compose the puzzle of my life every day from all over the world.

Thanks prof. Vianello for allowing me to be part of Lab45. Thank you, Manu, Luca, Vitto, Davide, Jessi and Max for introducing me to the pleasures of good music and good wine.

Thanks to who decided to stay. This is the beginning of new adventures.

